# The alkaline reaction of FEBEX bentonite: a contribution to the study of the performance of bentonite/concrete engineered barrier systems

## La reacción alcalina de la bentonita FEBEX: una contribución al estudio de la función de las barreras de ingeniería compuestas por hormigón y bentonita

J. Cuevas[1]*, R. Vigil de la Villa[1], S. Ramírez[2], L. Sánchez[1], R. Fernández[1], S. Leguey[1]

[1]*Universidad Autónoma de Madrid. Facultad de Ciencias. Departamento de Geología y Geoquímica. Ctra. de Colmenar km 15. 28049 Madrid, Spain*
[2]*Société ERM. SARL Études-Recherches-Matériaux. Bât. Géologie - 1er étage. 40, Avenue du Recteur Pineau. 86022 Poitiers Cedex, France.*

*e-mail adresses: jaime.cuevas@uam.es (*corresponding author), raquel.vigil@uam.es, susana.ramirez@erm-poitiers.fr., laura.sanchez@uam.es, raul.fernandez@uam.es, santiago.leguey@uam.es.*

Abstract

Since 1997, the development of two EU projects, Effects of Cement On CLAY barrier performance (ECOCLAY, 1997-2000 and ECOCLAY phase II (2000-2003; ANDRA, 2005), have addressed the effect of the alkaline plume induced by concrete on bentonite. The group working on applied clay geochemistry at the Autonomous University of Madrid (UAM) has participated in both projects, gaining experience on the Spanish reference bentonite. This paper deals with a synthesis of the work performed by the research group on FEBEX bentonite alkaline reactivity and the lessons learned for the performance assessment (PA) of the clay reference concept of deep geological repository for high level radioactive waste. The selected main scientific contributions to the performance assessment of this engineered barrier are: (1) the particular nature of FEBEX bentonite alkaline reaction products (zeolites, Mg-clays and CASH (calcium aluminate silicate hydrate phases); (2) the quantitative mineralogy approach to the rate of the high-pH reaction of FEBEX montmorillonite; and (3) the experimental validation of FEBEX bentonite alkaline reactivity in column experiments.

*Keywords*: bentonite, concrete, reactivity, waste disposal.

Resumen

Desde 1997, el desarrollo de dos proyectos de la Unión Europea, Effects of Cement On CLAY barrier performance (ECOCLAY, 1997-2000) y ECOCLAY phase II (2000-2003), ha permitido abordar la investigación del efecto de la pluma alcalina inducida por la lixiviación del hormigón sobre la bentonita. Ambos materiales forman parte de un concepto de barrera compuesta de hormigón y bentonita, en el contexto del almacenamiento de residuos a una profundidad dada. El grupo de geoquímica aplicada a las arcillas de la Universidad Autónoma de Madrid (UAM) ha participado en ambos proyectos, y ha conseguido aportar experiencia y conocimiento al estudio del comportamiento de la bentonita de referencia española (FEBEX) bajo condiciones de elevada alcalinidad. Este artículo ofrece una síntesis del trabajo desarrollado, mencionando las lecciones aprendidas sobre la reactividad alcalina de la

bentonita, y su enfoque práctico hacia el análisis del comportamiento de uno de los conceptos de referencia, el almacenamiento de residuos en formaciones arcillosas. Se han seleccionado las principales contribuciones científicas a este respecto, a juicio de los autores: (1) la naturaleza particular de los productos generados en la reacción alcalina de la bentonita FEBEX (zeolitas, arcillas magnésicas y geles de silicato aluminato cálcico hidratado (CASH)); (2) la aproximación mediante mineralogía cuantitativa al ritmo de reacción de la montmorillonita FEBEX a pHs elevados, y (3) la validación experimental de la reactividad alcalina de la bentonita a partir de experimentos en columna.

*Palabras clave*: bentonita, hormigón, reactividad, enterramiento de residuos.

## 1. Introduction

The study of the cement-bentonite interface reactivity is a key issue in the performance assessment of deep geological repositories for high level radioactive wastes (HLRW). Cement (in mortar or concrete) is used as an engineered barrier itself, for practical requirements in the construction of underground vaults, and in the final sealing of access routes (Glasser, 2001). Apart from engineering aspects, the concrete also functions as a solubility-limiting chemical alkaline environment for many radionuclides and posses a large sorption capacity for metal cations and possibly even for some anions and oxy-anions. The cement, held in contact with the bentonite barrier in the EBS (engineered barrier system), acts as a source of alkaline fluids in wet conditions. Then, an alkaline plume is expected to evolve at the interface with bentonite and may affect the clay barrier performance negatively. The key issue is thus to understand and possibly quantify the chemical processes and so assess their relevance to the performance assessment.

Since 1997, the development of two EU projects, Effects of Cement On CLAY barrier performance (ECOCLAY, 1997-2000; Huertas *et al*., 2000) and ECOCLAY phase II (2000-2003; ANDRA, 2005), have addressed the effect of the alkaline plume induced by concrete on bentonite. The group working on applied clay geochemistry at the Autonomous University of Madrid (UAM) has participated in both two projects, gaining experience on the Spanish reference bentonite FEBEX. This paper deals with a synthesis of the work performed by the research group on FEBEX bentonite alkaline reactivity and the lessons learned for the performance assessment (PA) of the clay reference concept of DGR-HLRW. Complementary work includes the studies conducted by the C.S.I.C. (Zaidín Group) on FEBEX-montmorillonite dissolution (Huertas *et al*., 2004) and that of C.S.I.C. (I. Eduardo Torroja) on the concrete performance aspects (Hidalgo *et al*., 2004).

The pH gradient developed at the concrete/bentonite interface can be described by examining the pH controls operating in each of the materials. Bentonite usually forms by hydrothermal alteration (< 100 ºC) of volcanic glass (Linares, 1987, and references therein). The reactions take place at near neutral pH conditions. In fact, the pH control in the bentonite can be explained mainly by the combination of the dissolution of the accessory mineral calcite and a cation exchange process that characterize its main mineralogical component, the montmorillonite (Bradbury and Baeyens, 2003; Fernández *et al*., 2004):

$$CaCO_3 + H^+ + 2NaX = HCO_3^- + CaX_2 + 2Na^+$$
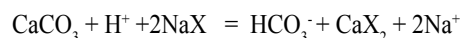
A range of pH values between 9 and 7 can be calculated if $P_{CO_2}$ is fixed at $10^{-3}$ bar and $a_{Na}^+$ varies between $10^{-3}$ to $10^{-1}$ M. These activities can be thought as the change in concentration that happens when bentonite is used in a compacted form, where the available free water for soluble salts decrease as well as pH does.

In contrast, the pH buffering in a concrete, made with an ordinary Portland cement (OPC) paste, is controlled by local equilibrium reactions, which operate as the concrete matrix is being leached by diluted groundwaters (Taylor, 1987; Glasser and Atkins, 1994; Faucon *et al*., 1998; Van Eijk and Brouwers, 2000). During concrete degradation, the pH of the leached pore-water may rise above 13.5 due to the release of potassium and sodium hydroxides. A typical composition of these early OPC concrete porewaters is a K/Na hydroxide ratio of 3/1, a pH >13, and saturation with respect to portlandite, $Ca(OH)_2$ (Berner, 1992; Andersson *et al*., 1989). When the alkali hydroxides have been leached, the pH is controlled by the dissolution of portlandite (pH = 12.5) and later, by the dissolution of calcium silicate hydrates or CSH gels of different Ca/Si molar ratios (1.7 - 0.6), in a pH range of 12.6 - 10. Ettringite (Aft) or monosulphate (Afm) are also dissolving during this stage.

Thus, the pH gradient at the studied interface is going to be affected by the interaction of pore-waters with the minerals that constitute both materials. Elevated temperatures will play a significant role in the system (due to radioactive decay), and can modify the rates of reaction as well as the nature of the resulting mineralogical mixture. Initially, the difference of pH between the two sides

of the interface ranges from five to six orders of magnitude in terms of proton or hydroxide concentration. This means that a high potential for diffusion and reaction exists at this interface.

The many studies performed on the alkaline reaction of bentonite have been directed, obviously, to the montmorillonite alteration. Previous studies on the reactivity of montmorillonite in alkaline solutions indicated the collapse of expandable smectite layers, in particular the formation of illite or illite/smectite mixed-layers. In Wyoming montmorillonite, Eberl *et al*. (1993) observed the increase of illite layers up to 25% after 9 months of reaction at 35 ºC in potassium hydroxide solution (KOH 3 M). In general, the formation of non-expanding layers depended on solution concentration rather than on the temperature and time of reaction. According to Bauer and Berger (1998), and Bauer and Velde (1999), the smectite reacts in potassium alkaline medium (KOH 4 M) up to 80 ºC to form an illite/smectite mixed-layer. However, formation of mixed-layer phases is an intermediate step in a series of dissolution-precipitation processes, including the formation of zeolite minerals. The pH and concentrations of these types of experiments largely exceeded the actual environments found in cement materials. The system will be influenced by the presence of portlandite $Ca(OH)_2$ and the alkali concentrations will be less than 1M. The use of more realistic conditions concerning the alkaline plume reactivity has been the choice for the investigations we are going to describe.

Among the montmorillonite alteration studies, few experimental studies have been done on reactive transport processes affecting compacted bentonite. The experiments performed by the UAM group during ECOCLAY were, to our knowledge, the first ones, followed by those of Nakayama *et al*. (2004). These authors have shown an increase of porosity and permeability in compacted bentonite, in contact with a highly alkaline (NaOH, pH = 14) solution due to montmorillonite dissolution.
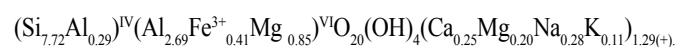
When two porous media, like concrete and clay, act as fluid transport pathways, the evolution of porosity is dependent on the dominant reactive transport process. For instance, porosity reduction is predicted in the reacted clay matrix by means of a diffusion-reaction process (Savage *et al*., 2002; De Windt *et al*., 2004). This fact has been experimentally observed in claystone by Read *et al*. (2001) or Adler (2001). In contrast, advective-dominated transport will increase the porosity (Steefel and Lichtner, 1994). More complexity can be added if one takes into account that the nature of the secondary minerals will be strongly affected by the cationic content of reactive fluids and the pH (i.e., Chermak, 1992; Vigil de la Villa *et al*., 2001; Ramírez *et al*., 2005).

This paper will show the more relevant results obtained on alkaline alteration of FEBEX bentonite either by means of static alteration experiments (batch tests) or dynamic ones (transport cell tests), including as variable factors, as the chemistry of alkaline solutions, bentonite density, and temperature and time.

## 2. Experiments performed

In order to study both reactivity and alteration, in terms of affected thickness of the compacted clay barrier, two types of experiments were designed. The bentonite reactivity was provoked by mixing the clay and the alteration solutions in hermetic batch reactors at different temperatures during periods of up to 18 months. These studies of reactivity were always complemented by the implementation of permeability cell experiments considering the intrusion of either neutral (granitic) or alkaline solutions through OPC cement mortars held in contact with compacted bentonite. Figure 1 shows a general picture of the overall physicochemical conditions and experimental devices used in the experiments.

All the tests performed on the FEBEX bentonite during the ECOCLAY projects were prepared with a bentonite from La Serrata of Níjar (Almería, Spain). The bentonite used was from the "Cortijo de Archidona" deposit (Caballero *et al*., 1983; Caballero *et al*., 2005). The bentonite was comprised of 93 ± 3 % montmorillonite, 2 ± 0.5 % quartz, 2 ± 1 % potassium feldspars, 1 ± 0.7 % plagioclase, 2 ± 0.2 % cristobalite, 1 ± 0.7 % calcite and 1.5 ± 0.1 % rhyodacitic precursor rock, mainly as volcanic glass (Cobeña *et al*., 1998; Linares *et al*., 1993). The < 0.5 µm fraction was comprised of a mixed-layer I/S with 90% of montmorillonite layers (Ramírez *et al*., 2002; Cuadros and Linares, 1995). The average structural formula of the clay after $Ca^{2+}$ saturation is:

$$(Si_{7.72}Al_{0.29})^{IV}(Al_{2.69}Fe^{3+}_{0.41}Mg_{0.85})^{VI}O_{20}(OH)_4(Ca_{0.25}Mg_{0.20}Na_{0.28}K_{0.11})_{1.29(+)}.$$

The distribution of exchangeable cations ($Ca^{2+}$, $Mg^{2+}$, and $Na^+$) has been calculated by extracting the exchageable cations by a standard chemical method (Thomas, 1982). Their atomic proportions can be fixed by knowing the average total layer charge after the chemical analysis of a $Ca^{2+}$ saturated clay sample. $K^+$ in the formula is irreversibly fixed. This is in agreement with the presence of non-expandable layers as detected by XRD measurements. The determined CEC of the < 0.5µm size fraction, at pH = 7, is 122 (±5) cmol(+)/kg (air dried weight basis: Huertas *et al*., 2000). Taking into account that the molecular weigth of the FEBEX montmorillonite is 753.8 (oven dry basis), and that approximately a 15 % water content is bound to the air dried clay material, the cal-

## EXPERIMENTAL DESIGN

**Granitic/alkaline water
1 MPa**



batch reactors
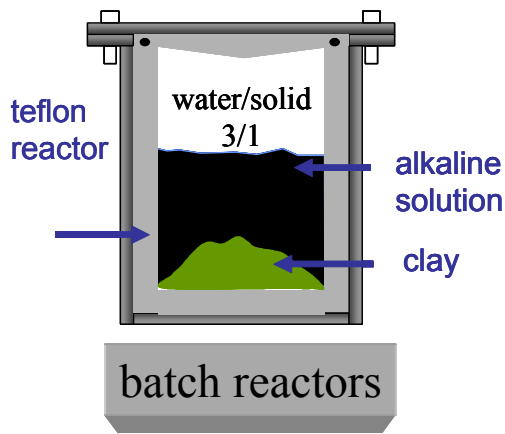
$NaOH/KOH/Ca(OH)_2$
pH= 10 - 13.5
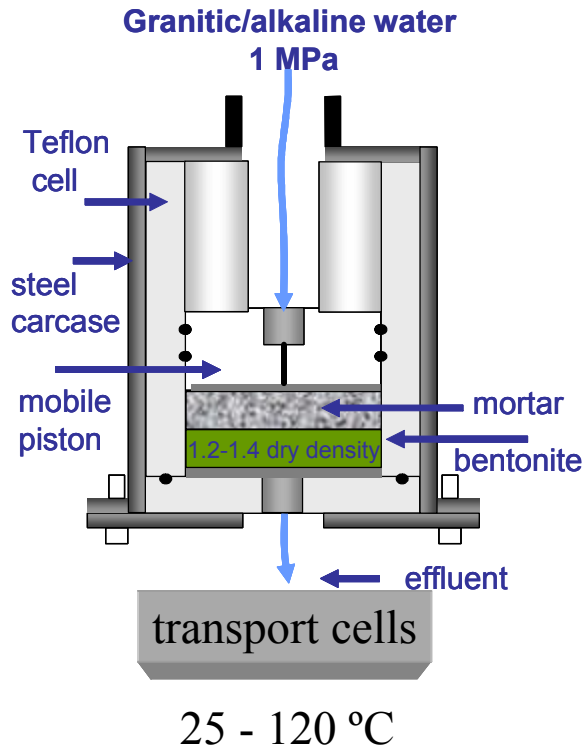25 – 200 ºC

transport cells

25 - 120 ºC

Fig. 1.- Sketch of experimental devices and range of conditions used in the FEBEX bentonite alkaline reactivity investigations.
Fig. 1.- Esquema de los dispositivos y rango de condiciones experimentales utilizados en las investigaciones sobre la reacción alcalina de la bentonita FEBEX.

culated CEC (Ca, Mg and Na) is 133 cmol(+)/kg. The excess respecting measured CEC can be attributed to the variable charge contribution, as far as the saturation of the analyzed clay was not pH buffered.

The cement used in the experiments was an Ordinary Portland Cement (OPC-CEM-I) provided by the IETcc-CSIC cement group, whose composition, once hydrated, is detailed in Table 1 (Hidalgo *et al*., 2003). The percentages are shown in ranges, because the solid phases that compose it are heterogeneous, sometimes amorphous, and their characterization and quantification proved to be difficult. In these experiments, cement material (mortar:

| Phases | CEM-I (% in weight) |
|---|---|
| Calcium Silicate Hydrate (CSH) | 40 - 60 |
| Portlandite (Ca(OH)$_2$) | 20 - 25 |
| Monosulphate and ettringite phases | 10 - 20 |
| Pore solution | 10 - 20 |
| NaOH, KOH, Mg(OH)$_2$ | 0 - 5 |

Table 1.- Range of phase abundances in fully hydrated CEM-I Portland cements (Hidalgo *et al*., 2003).
Tabla 1.- Rango de abundancia de fases en cementos Portland CEM-I completamente hidratados (Hidalgo *et al*., 2003).

quartz sand + cement: 3 + 1; and water/cement ratio 0.45) was required (1) to perform as a permeable medium to allow an advective alkaline flow to pass through the cement-bentonite columns; and (2) to provide a potential and realistic source of calcium in order to allow cation exchange and to study its spatial evolution in the bentonite segment.

### 2.1. Batch experiments

#### 2.1.1. Alkali hydroxide solutions

In a first approach to the alkaline reactivity, batch experiments were run with bentonite (as bulk sample or separated < 2 μm fraction) and alkaline solutions (Table 2) from 7 days up to 365 days at 35, 60 and 90 ºC. The solid/solution ratio was 1/3, 80 g of bentonite and 240 ml of solution or 10 g of the < 2 μm fraction and 30 ml solution. The experimental parameters are shown in Table 3.

In both initial and treated samples, mineralogy was studied by X-ray diffraction (XRD) and scanning electron microscopy (SEM) equipped with energy dispersive X-ray analyzer (EDX). The concentration of the exchangeable cations was determined after the tests by NH$_4$-OAc displacement at pH = 8 (Thomas, 1982), and the < 0.5

| solu-tion | $Na^+$ (mol/dm³) | $K^+$ (mol/m³) | $Ca^{2+}$ (mmol/dm³) | pH |
|---|---|---|---|---|
| a | - | - | 22.3 | 12.6 |
| b | 0.08 | 0.17 | 0.852 | 13.2 |
| c | 0.17 | 0.33 | 0.407 | 13.5 |
| d | 0.0001 | - | - | 10.0 |
| e | 0.10 | - | 2.4 | 12.9 |
| f | 0.50 | - | 0.41 | 13.5 |
| g | - | 0.10 | 2.4 | 12.9 |
| h | - | 0.50 | 0.41 | 13.5 |

Table 2.- Chemical composition of the initial alkaline solutions used in the Ecoclay (1997-2000) project (Ramírez *et al*., 2002).

Tabla 2.- Composición química de las soluciones alcalinas iniciales utilizadas en el proyecto Ecoclay (1997-2000) (Ramírez *et al*., 2002).

| sample | solution | t (days) | T (ºC) |
|---|---|---|---|
|  | a | 30, 90, 180, 365 | 35, 60, 90 |
| bentonite | b | 30, 90, 180, 365 | 35, 60, 90 |
|  | c | 30, 90, 180, 365 | 35, 60, 90 |
|  | d | 30, 90, 180, 365 | 35, 60, 90 |
|  | e | 7, 30, 90 | 35, 60, 90 |
| < 2 mm | f | 7, 30, 90 | 35, 60, 90 |
| fraction | g | 7, 30, 90 | 35, 60, 90 |
|  | h | 7, 30, 90 | 35, 60, 90 |

Table 3.- Experimental conditions of the tests performed during the Ecoclay (1997-2000) project (Ramírez *et al*., 2002).
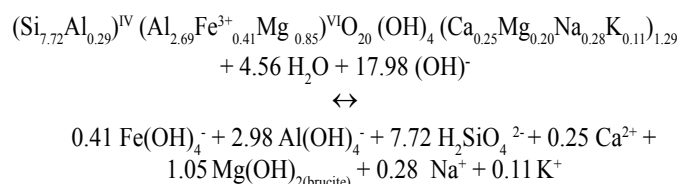
Tabla 3.- Condiciones experimentales de los ensayos realizados durante el proyecto Ecoclay (1997-2000) (Ramírez *et al*., 2002).

μm fraction saturated in $Ca^{2+}$ was studied by XRD and chemical analysis in order to calculate the average structural formulae of altered smectite.

*Geochemical controls in the aqueous phase*

One of the most important observations made during the interaction between alkaline solutions and bentonite was that montmorillonite can be considered as an important buffer agent of the pH in the bentonite, since the pH values decreased in a similar fashion in the < 2 μm fraction tests (pure montmorillonite) or in the bulk bentonite tests (Ramírez *et al*., 2002). The pH decrease is mainly due to the dissolution of montmorillonite and the deprotonation of aqueous silica (i.e. $H_4SiO_4 \rightarrow H_2SiO_4^{2-} + 2 H^+$), and also to the incorporation of $OH^-$ in the structure of newly-formed minerals or the retention of $OH^-$ in the external surface of smectite may play a significant role (Stumm, 1992; Dove, 1995). The dissolution of FEBEX

montmorillonite can be described as (modified from Cama *et al*., 2000):

$$(Si_{7.72}Al_{0.29})^{IV} (Al_{2.69}Fe^{3+}_{0.41}Mg_{0.85})^{VI}O_{20} (OH)_4 (Ca_{0.25}Mg_{0.20}Na_{0.28}K_{0.11})_{1.29}$$
$$+ 4.56\, H_2O + 17.98\, (OH)^-$$
$$\leftrightarrow$$
$$0.41\, Fe(OH)_4^- + 2.98\, Al(OH)_4^- + 7.72\, H_2SiO_4^{2-} + 0.25\, Ca^{2+} +$$
$$1.05\, Mg(OH)_{2(brucite)} + 0.28\, Na^+ + 0.11\, K^+$$

Brucite is used for magnesium instead a soluble form, as far as at pH > 12, the solutions did not contained detectable amounts for this cation.

Figure 2 shows the typical pH decrease observed in the batch experiments, in agreement with this reaction. When the initial solutions were either $Ca(OH)_2$ saturated (solution **a**; pH = 12.5) or $10^{-4}$ mol/dm³ NaOH (solution **d**; pH =10), the buffering capacity of the bentonite fixes the pH at $8.0 \pm 0.3$ in the range of 35-90 ºC. This pH characterizes the equilibrium pH of the bentonite porewater itself influenced by the presence of small amounts of calcite. In fact, the alkalinity is completely determined by the carbonate chemical system. However, higher initial pH values result in more alkaline final solutions. It becomes thus clear that the use of a single step batch reaction of bentonite with a portlandite saturated solution is not suitable to resemble a $Ca(OH)_2$ cement source.

Other chemical changes observed in the bentonite high-pH interaction solutions can be summarized as follows with regard to the initial composition (Huertas *et al*., 2000):

• incorporation of carbonic species due to the calcite dissolution

• relative decrease of the concentration of the major cations, $Na^+$ and $K^+$, in the pH > 13 tests, due to the cation exchange.

• approximately fixed concentrations of $Ca^{2+}$ and $Mg^{2+}$ ($< 10^{-3}$ M)

• increase of the dissolved silica. The concentration depended on the pH and on the dissolution of volcanic glass. At pH = 13.5, the concentration is $2\cdot10^{-2}$ M in the reactions with bentonite and $1\cdot10^{-2}$ M in the reactions with montmorillonite. The temperature (90 – 35 ºC) does not influence this in a significant way.

*Geochemical reactivity of bentonite minerals*

Zeolite crystallization and magnesium increase in the averaged calculated octahedral sheet of the smectite composition are the main signatures of the transformation of FEBEX bentonite when exposed to alkali-hydroxide solutions and moderated temperatures. However, the bentonite remained virtually unchanged because newly-formed minerals constituted < 5 % of the bulk mass of treated bentonite.
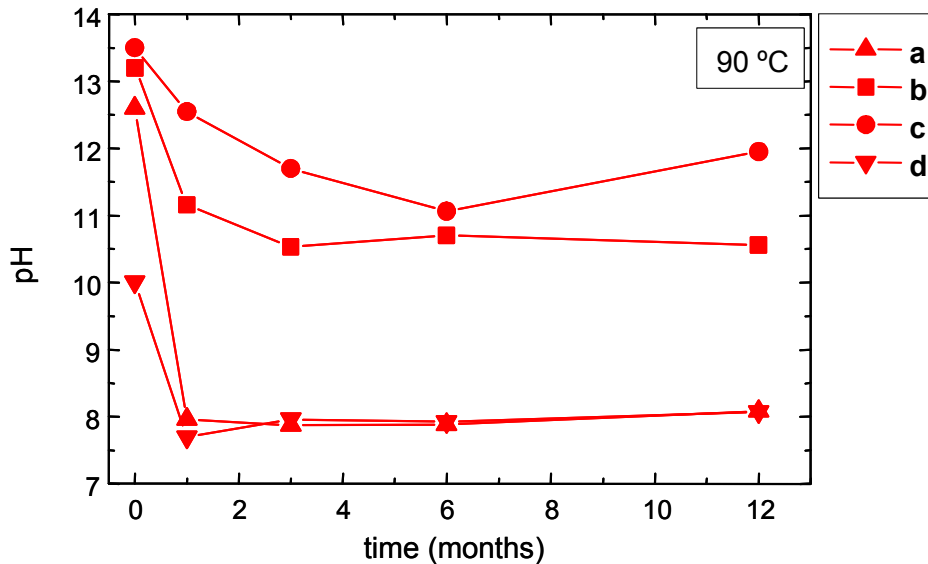
Fig. 2.- pH buffering of FEBEX bentonite at 90 ºC.
Fig. 2.- Tamponamiento del pH de la bentonita FEBEX a 90ºC.

The zeolite formation (phillipsite type) was detected by XRD and SEM-EDX in the tests with bentonite at 35 - 90 ºC and in the tests with montmorillonite at 90 ºC after 12 months or 12 weeks, respectively. In the former experiments, the zeolites appear in the samples treated with 0.5 M sodium-potassium solution (pH = 13.5). In the latter, the zeolites are only detected in the montmorillonite treated with the 0.5 M sodium solution (pH = 13.5).

The chemical composition of the produced phillipsite includes sodium, potassium and magnesium:

$(Na_{2.48}K_{1.24}Ca_{0.18}Mg_{0.58})\ (Al_{4.83}Fe_{0.07}Ti_{0.04})\ Si_{10.97}\ O_{32}$
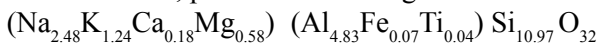
The formation of zeolite type analcime is detected also by XRD in the montmorillonite treated with the 0.5 M sodium solution, at 90 ºC after 12 weeks. Figure 3 shows the phillipsite morphology and the XRD powder diffraction profiles from montmorillonite alteration.

The increase of pH and temperature, the existence of volcanic glass and longer times favoured the process of zeolites formation. Moreover, the type of zeolite formed will depend critically on solution composition and temperature. Figure 4 (Vigil *et al*., 2001) demonstrated the thermo-chemical consistency of the experimentally produced mineral phases.

The incorporation of $Mg^{2+}$ into the solid phase was inferred in view of the decrease of $Mg^{2+}$ in the exchange complex and from the low concentration of $Mg^{2+}$ in the reacted waters. The incorporation of $Mg^{2+}$ into the solid phase is favoured by the increase of the pH, of the temperature and of the time of treatment in the same fashion as zeolite formation.  Figure 5 illustrates the relationship between the displacement of $Mg^{2+}$ from the exchange complex and the increase of octahedral $Mg^{2+}$ in the calcu-

lated montmorillonite structure. Montmorillonite formulas were calculated using a previously homoionized($Ca^{2+}$) clay, avoiding any confusion between octahedral and exchangeable magnesium.

Two main questions arouse from these first experiments: (1) could we better understand the reaction by increasing temperature in order to achieve a higher degree of progress?; and (2) can we better approximate the OPC cement/bentonite interaction by including solid $Ca(OH)_2$ in the batch reactors?

The first stages of interaction at the cement-bentonite interface will be characterized by significant amounts of portlandite in contact with alkali-hydroxide solutions and bentonite. Thus, a comprehensive study of this system has to take into account these phases as shown by Savage *et al*. (1992; 2002) in modelling calculations. On the other hand, we have shown that the alkaline reaction of FEBEX bentonite is significantly accelerated with the increase in time and temperature (Ramírez *et al*., 2002). Thus, our contribution to the Ecoclay-II project (2000 – 2003) was devoted to focus on the above-mentioned questions.

### 2.1.2. Alkali hydroxide solutions considering the portlandite interface

Our second approach to the alkaline reactivity incorporated portlandite and considered higher temperatures. The bentonite (80g) and three alkaline solutions (0.240 L: 0.1, 0.25 and 0.5M NaOH; pH: 12.90, 13.26 and 13.52 after speciation) were mixed. The system was initially buffered at portlandite saturation by including an excess of portlandite (6 g: about 4 times the cation exchange capacity CEC of the bentonite ($100 \pm 2$ cmol (+)/kg)) in the
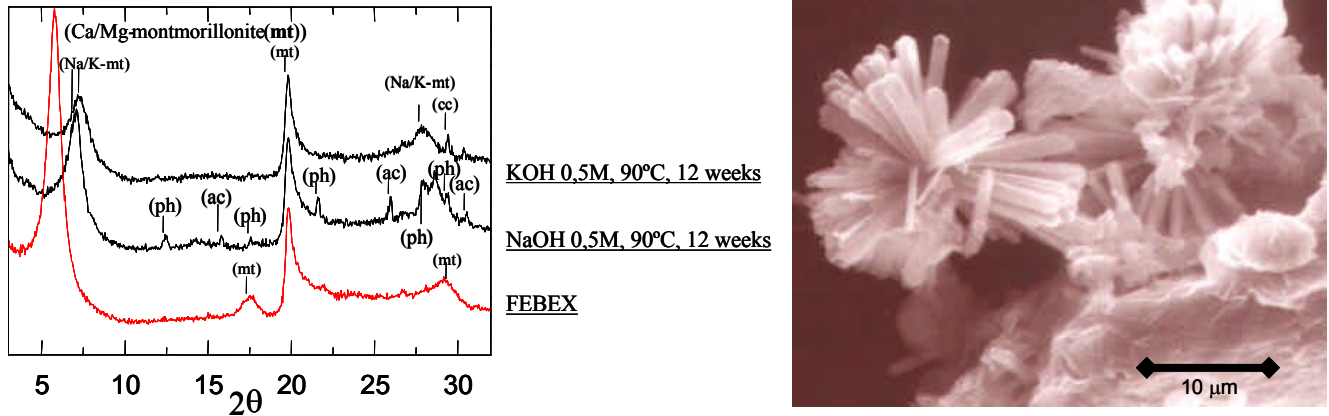
Fig. 3.- Zeolite morphology formed in the reactions with bentonite at 60 ºC. XRD powder diffraction profiles comparing reacted and untreated FEBEX montmorillonite. ph: phillipsite, ac: analcime, Na/K-mt: Na/K-montmorillonite, cc: calcite.

Fig. 3.- Morfología de zeolita formada en las reacciones con bentonita a 60ºC. Perfiles de difracción de rayos X comparando montmorillonita FEBEX sin tratar y después de la reacción alcalina. ph: filipsita, ac: analcima, Na/K-mt: Na/K-montmorillonita, cc: calcita.
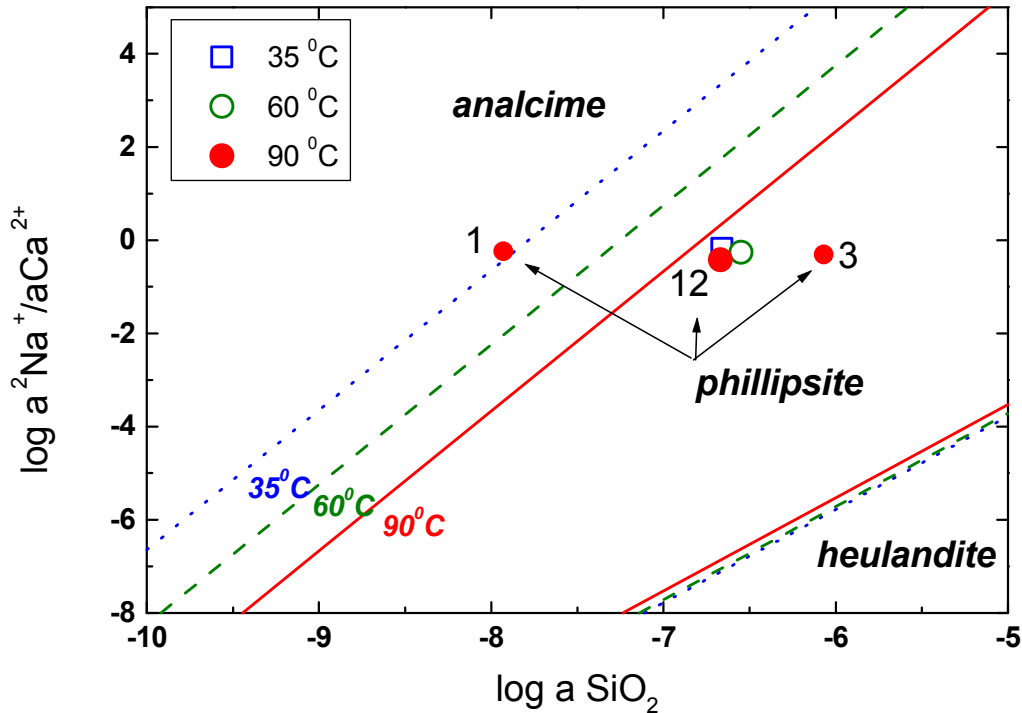


Fig. 4.- Activity-activity-ratio plot of the final conditions of the 1, 3 and 12 months experiments of FEBEX bentonite mixed with solution c (Table 1). The stability fields were calculated by Vigil *et al*. (2001) for zeolite minerals, using thermo-chemical data from Chipera and Bish (1997).

Fig. 4.- Gráfico de relación actividad-actividad de las condiciones finales de los experimentos a 1, 3 y 12 meses de la bentonita FEBEX mezclada con la solución c (Tabla 1). Los campos de estabilidad fueron calculados por Vigil *et al*. (2001) para zeolitas, usando datos termo-químicos de Chipera y Bish (1997).

reactor. The experimental t/T grid was 1, 6, 12 and 18 months and 25, 75, 125 and 200 ºC.

*Geochemical controls in the aqueous phase*

As in the other batch experiments, bentonite was able to buffer the alkaline solutions at stationary (540 days) values between pH 12.5 and 8.5 depending on temperature and initial NaOH concentration (Table 4, Cuevas, 2005). The rise in temperature favored neutralization of the initial hydroxide alkalinity.

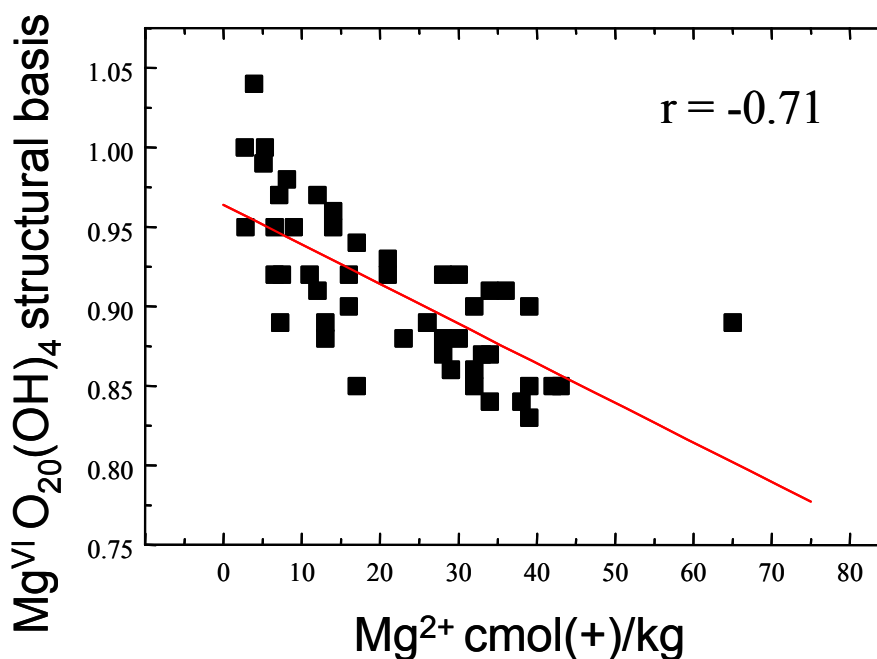Despite the addition of $Ca(OH)_2$ or the complete depletion of magnesium in the exchange complex which was

Fig. 5.- Linear relationship between the average octahedral $Mg^{2+}$ in montmorillonite and the exchangeable $Mg^{2+}$ in the bentonite tests. Exchangeable $Mg^{2+}$ expressed as positive charge moles relative to mass units.

Fig. 5.- Relación linear entre la media de $Mg^{2+}$ octaédrico en la montmorillonita y el $Mg^{2+}$ intercambiable en los ensayos de bentonita. El $Mg^{2+}$ intercambiable está expresado como moles de carga positiva relativa a unidades de masa.

observed in all the experiments performed, alkaline-earth cations exhibited less than 1 mmol/l concentration, so that they were again incorporated into the solid phases. In fact, the characteristics of the aqueous solution components were very similar to the previous experiments, except for the case of silica. A clear dependency on pH or temperature was not apparent, keeping in mind that the silica concentration should rise as pH or temperature are increased. Its concentration ranged from 1 to 5 mmol/l,

| T | Stationary pH | | % transformed smectite (XRD) (540 days) |
|---|---|---|---|
| Initial conditions | 13.5 (0.5 M NaOH) | 12.9 (0.1M NaOH) | 0.5 M NaOH – 0.1 M NaOH |
| 25 ºC | 12.5 | 12.0 | 4.5 - 3.0 |
| 75 ºC | 12.0 | 11.5 | 7.5 – 4.0 |
| 125 ºC | 10.5 | 10.0 | 19.0 – 9.5 |
| 200 ºC | 9.5 | 8.5 | 36.0 – 17.5 |

Table 4.- Maximum values for smectite transformation under the experimental conditions used for the of Ecoclay-II experiments (2000-2003).

Tabla 4.- Valores máximos para la transformación de esmectita bajo las condiciones experimentales utilizadas para los experimentos de Ecoclay-II (2000-2003).

which is significantly lower than observed in the previous high pH experiments performed without portlandite that showed higher silica concentrations (> 10-20 mmol/l). This suggests that the formation of calcium silicates will play an important role in the control of aqueous silica. This fact can be thoroughly demonstrated by chemical equilibrium calculations (Fig. 6, Cuevas *et al.*, 2006).

*Geochemical reactivity of bentonite minerals*

XRD analysis of reacted-bentonite showed mainly the formation of analcime (ideally $(Na_2,Ca)\,Al_2Si_4O_{12}\cdot 2H_2O$) and 11 Å- tobermorite ($Ca_5Si_6O_{16}(OH)_2\cdot 4H_2O$)) at 200-125 ºC in all tests. At lower temperatures and at lower pH, amorphous calcium hydrated silicates (CSH-gel) is presumed to have formed because neither portlandite ($Ca(OH)_2$) nor nanocrystalline-CSH (3.07 Å) are evident in XRD spectra (Fig. 7). Moreover, the smectites became significantly transformed, as can be deduced from the loss of intensity in the 4.45 Å peak when the patterns are plotted after background normalization, even if no crystalline secondary phases have been formed. As seen in Table 4, the progress of reaction was far more advanced than in the previous experiments.
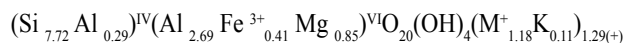
Figure 8 shows several photographs of the main newly-formed minerals obtained by SEM microscopy. The detailed composition of analcime and CSH phases were in-
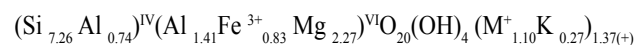
vestigated by SEM-EDX, although some variability was found related to their ideal compositions, its description is beyond the scope of this paper (see Cuevas, 2005).

Smectites were the only clay minerals detected in the 0.5 μm size fraction after the tests by means of XRD. However, there were visible changes in their structural characteristics outlined in the most alkaline tests. A 1.53 Å peak evidenced the presence of a new tri-octahedral smectite when alkalinity or temperature rose (Fig. 9). The nature of this phase has been determined as saponitic (tetrahedral charged tri-octahedral smectite). This is demonstrated by the significance of $^{IV}Al$ (tetrahedral) positions and Si-2Si1Al atomic environments, by means of $^{29}Si$ and $^{27}Al$ MAS-NMR (Fig. 10, Cuevas *et al.*, 2004). This atomic environment (one Si surrounded by one Al and two other Si) was not visible in the original montmorillonite, now indicating a major contribution of tetrahedral charge to the total layer charge. Furthermore, these data are in close agreement with the structural formula calculations made on the most altered samples (540 days, pH =13.5, 200 ºC):

*initial*

$$(Si_{7.72}Al_{0.29})^{IV}(Al_{2.69}Fe^{3+}_{0.41}Mg_{0.85})^{VI}O_{20}(OH)_4(M^+_{1.18}K_{0.11})_{1.29(+)}$$

*altered*

$$(Si_{7.26}Al_{0.74})^{IV}(Al_{1.41}Fe^{3+}_{0.83}Mg_{2.27})^{VI}O_{20}(OH)_4(M^+_{1.10}K_{0.27})_{1.37(+)}$$

This increase of octahedral Mg (towards a tri-octahedral composition) can be considered enormous in comparison with the experiments performed up to 90 ºC, in which the measured change was < 0.1 atoms per formula unit (Fig. 5).

### Kinetics of montmorillonite transformation

Once the nature of the alkaline reaction of bentonite had been studied in detail, the rate of montmorillonite transformation was calculated by using the mineralogical quantification of smectite (calibrated by the decrease of the 4.45 Å XRD peak area) in the 75 – 200 ºC tests. The trend is poorly defined at lower temperatures (Fig. 11).

The kinetics of mineral formation (zeolites and saponite) and smectite transformation were evaluated as a function of OH$^-$ concentration. Unfortunately, the formation of CSH-gel is difficult to evaluate kinetically. We know that all the portlandite has been transformed but we do not know the exact phases that have been formed. We therefore presume that the CSH-gel has formed instantaneously at the time scale of the experiment (Cuevas,
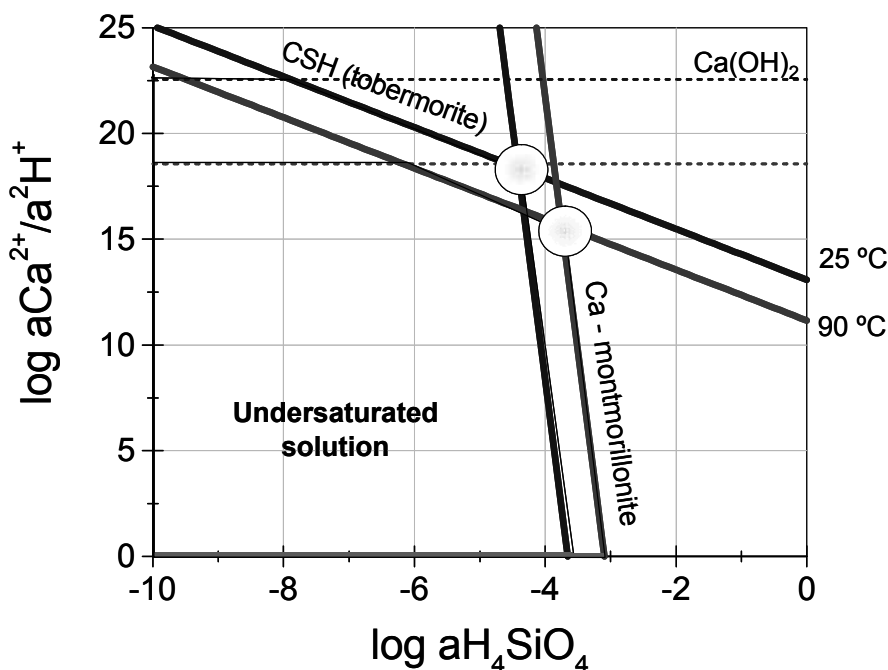


Fig. 6.- Stability diagram calculated for calcium silicate hydrate (CSH, 11 Å tobermorite, $Ca_5Si_6O_{16}(OH)_2(H_2O)_{4.5}$) and Ca-montmorillonite ($Ca_{1/6}Mg_{1/3}Al_{5/3}Si_4O_{10}(OH)_2$) in equilibrium at 25-90 ºC. Al and Mg soluble species are considered to be in equilibrium with gibbsite and brucite, respectively. The chemical composition and thermodynamic data of the two phases have been taken from Wolery (1998) EQ3/6 V7-REL-V6.2c LLNL alt database.

Fig. 6.- Diagrama de estabilidad calculado en equilibrio a 25-90ºC para silicato de calcio hidratado (CSH, 11Å tobermorita, $Ca_5Si_6O_{16}(OH)_2(H_2O)_{4.5}$) y montmorillonita cálcica ($Ca_{1/6}Mg_{1/3}Al_{5/3}Si_4O_{10}(OH)_2$). Las especies solubles de Al y Mg se consideran en equilibrio con gibsita y brucita, respectivamente. La composición química y los datos termodinámicos de las dos fases se han tomado de la base de datos de Wolery (1998) EQ3/6 V7-REL-V6.2c LLNL.
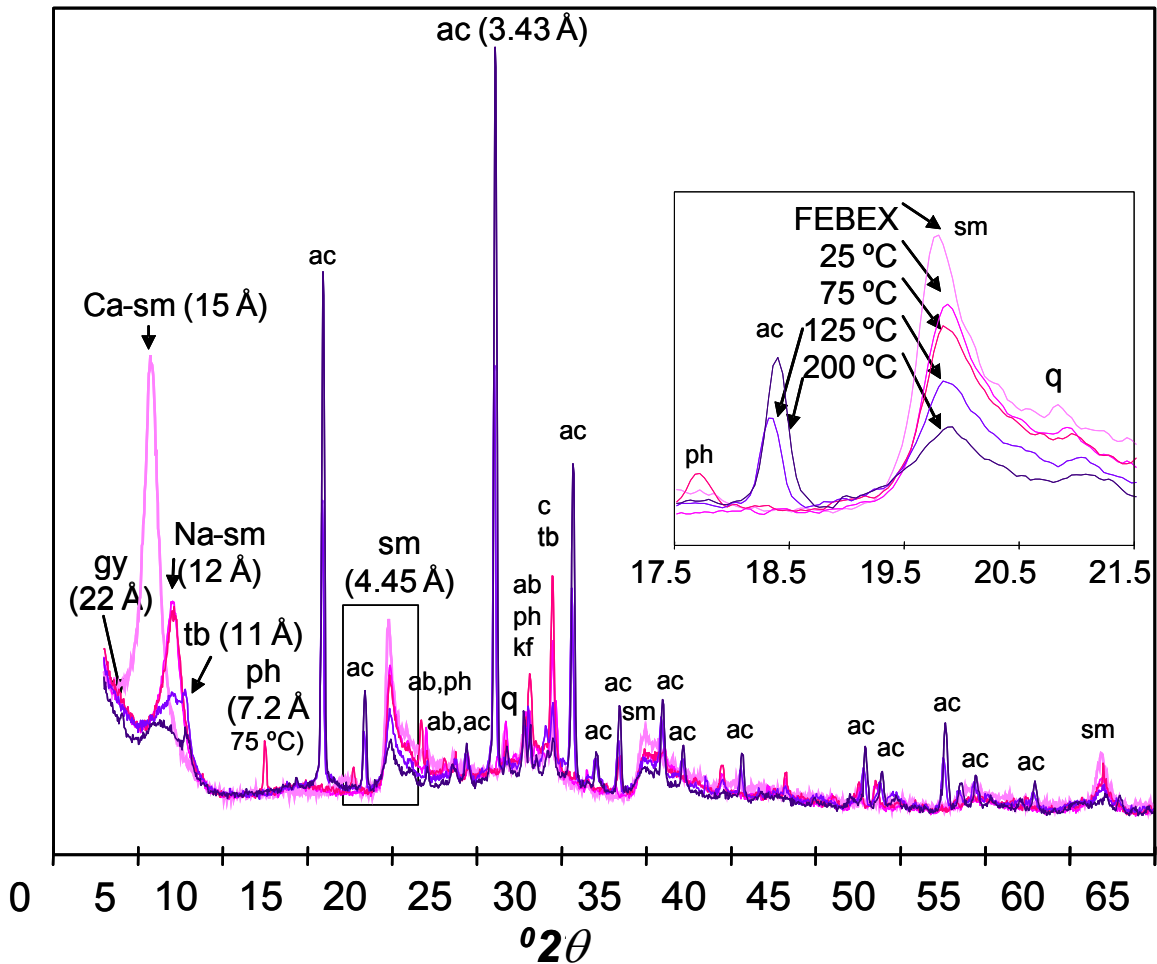
Fig. 7.- XRD Background normalized patterns (random powder) of altered bentonites at 540 days, (NaOH 0.5 M). Ca-sm: Ca-smectite, sm: smectite, Na-sm: Na-smectite, ac: analcime, ph: phillipsite, tb: tobermorite, gy: gyrolit, q: quartz, ab: albite, kf: K-feldspar, c: calcite.

Fig. 7.- Patrones normalizados de XRD (polvo) de bentonitas alteradas a 540 días (NaOH 0.5M). Ca-sm: esmectita cálcica, sm: esmectita, Na-sm: esmectita sódica, ac: analcima, ph: filipsita, tb: tobermorita, gy: girolito, q: cuarzo, ab: albita, kf: feldespato potásico, c: calcita.

2005).

The kinetics for the conversion of montmorillonite can be fitted to R (mol·s$^{-1}$) = A (m$^2$)·k [OH$^-$]$^{0.5}$ , with ln k = (-20.09 ± 1.37) – (2731 ± 543) * (1/T). The activation energy that describes the temperature dependence of the rate is E$_a$ = 22.7 ± 4.4 KJ/mol. (Fig. 12).

It is clear that a slight increase of the order of reaction at low temperature is observed (Table 5). Some authors (Huertas *et al.*, 2004) consider the reaction order to vary with temperature, but in our complex system (several minerals involved in dissolution-precipitation reactions), apparent changes on the order of reaction can be attributed to the overlapping of several global reactions. On the other hand, these results are comparable to those obtained in previous studies for the dissolution of montmorillonite alone. Our rate constant is lower, and the order of reaction is slightly higher than the data from Bauer and Berger (1998) or Huertas *et al.* (2004). However, they find **n** close to 0.3, the same value as suggested by our high temperature experiments. Nakayama *et al.* (2004) have

| T | k | N | Chi^2 |
|---|---|---|---|
| 75 ºC | 7.6 E-13 ± 1 E-13 | 0.65 ± 0.14 | 2.8 E-27 |
| 125 ºC | 2.5 E-12 ± 6 E-14 | 0.52 ± 0.02 | 9.7 E-28 |
| 200 ºC | 4.2 E-12 ± 9 E-13 | 0.32 ± 0.12 | 4.7 E-25 |

| T | k | n | |
|---|---|---|---|
| 75 ºC | 6.5 E-13 ± 8 E-14 | 0.50 | |
| 125 ºC | 2.5 E-12 ± 3 E-14 | 0.50 | |
| 200 ºC | 5.2 E-12 ± 7 E-13 | 0.50 | |

Table 5.- Curve fitting parameters for the reaction rate (R) for montmorillonite conversion (R/A = k [OH$^-$]$^n$). The data were alternatively fitted with n = 0.5 in order to perform more consistent apparent activation energy calculations.

Tabla 5.- Parámetros de ajuste de la curva para la tasa de reacción (R) para la transformación de la montmorillonita (R/A = k [OH$^-$]$^n$). Los datos se ajustaron alternativamente con n = 0.5 para realizar cálculos de energía de activación aparente más consistentes.
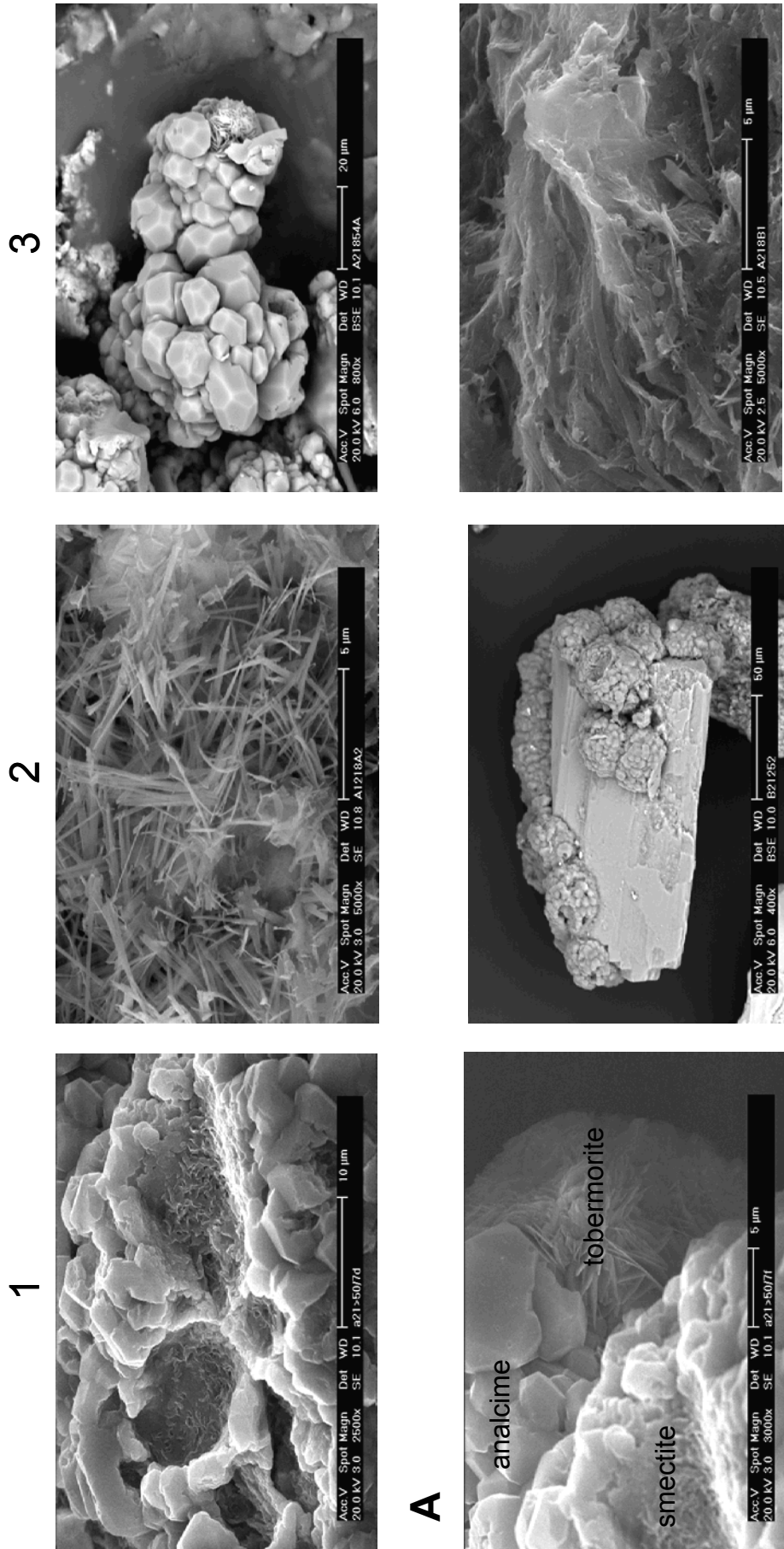
Fig. 8.- SEM aspects of newly formed minerals. 1A: analcime on smectite. 0.5 M NaOH, 200 °C, 30 days. 2A: gel-CSH (disordered), 0.5 M NaOH, 125 °C. 540 days. 3A: analcime, 0.5 M NaOH, 200 °C, 540 days. 1B: coexistence of analcime, smectite and a tobermorite, 0.5 M NaOH, 200 °C. 30 days. 2B: analcime supported on plagioclase, 0.25 M NaOH, 200 °C, 360 days. 3B: fibrous clay matrix: 0.5 M NaOH, 200 °C, 540 days.

Fig. 8.- Aspecto bajo el microscopio electrónico de barrido de los minerales de nueva formación. 1A: analcima sobre esmectita. 0.5 M NaOH, 200 °C, 30 días. 2A: gel-CSH (desordenado), 0.5 M NaOH, 125 °C. 540 días. 3A: analcima, 0.5 M NaOH, 200 °C, 540 días. 1B: coexistencia de analcima, esmectita y tobermorita, 0.5 M NaOH, 200 °C. 30 días. 2B: analcima sobre plagioclasa, 0.25 M NaOH, 200 °C, 360 días. 3B: matriz de arcilla fibrosa: 0.5 M NaOH, 200 °C, 540 días.
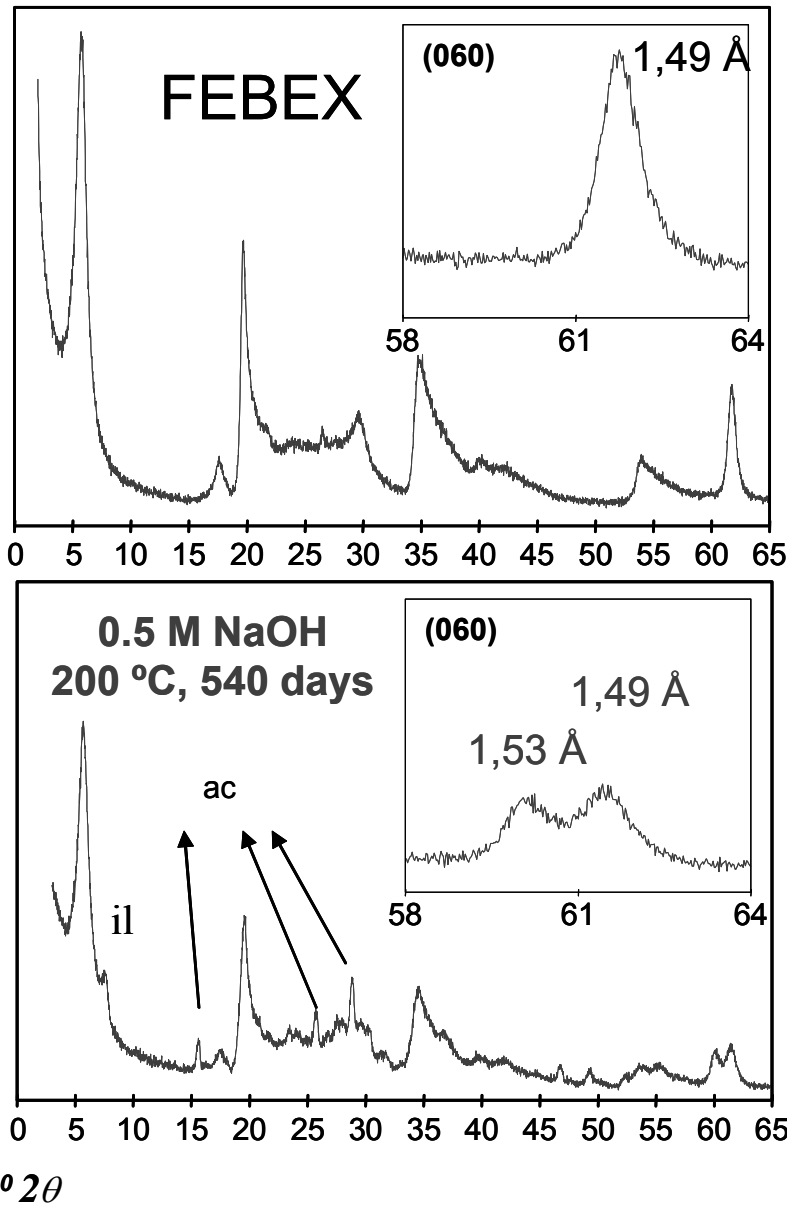
Fig. 9.- XRD patterns (< 0.5 µm separated samples) showing extreme alteration effects. Random powder patterns and (060) angle region. Il: illite, ac: analcime.
Fig. 9.- Espectro de XRD (muestras separadas <5 µm) mostrando efectos de alteración extrema. Diagramas de polvo y región (060). Il: illita, ac: analcima.

shown that in column experiments with sand-bentonite mixtures, reaction rates at 1 M Na-K-OH solutions ($pH_{25}$ ºC = 14) are one order of magnitude lower than Bauer and Berger's work, indicating that higher solid to solution ratios in compacted bentonite will diminish the reaction rates.

## 2.2. Permeability cell experiments

### 2.2.1. Composite mortar/low density compacted bentonite (1.2 g/cm³ dry density)

The objective of the first column experiments carried out in the UAM group was to study the mineralogical, the microstructural and the physico-chemical changes in the bentonite as a result of their interaction with the cement

pore waters in an open system. The tests were performed in permeability cells, where the cement mortar (1.5 cm thickness) and the compacted FEBEX bentonite (1.5 cm thickness, dry density of 1.2 g/cm³) were introduced. A flow of water of granitic composition (Table 6) passed through the cells injected at a pressure of 1 MPa (see Fig. 1).

The main variables of the tests were the temperature (35, 60 and 90 ºC) and time (1, 6 and 12 months). Two very similar cement types were used (CEM-I and CEM-I-SR, Huertas *et al.*, 2000), but virtually no influence was detected on bentonite alteration due to the different compositions. Here, we will show the main effects detected concerning transport (permeability), pH buffering of the alkaline plume and the spatial pattern of bentonite alteration.
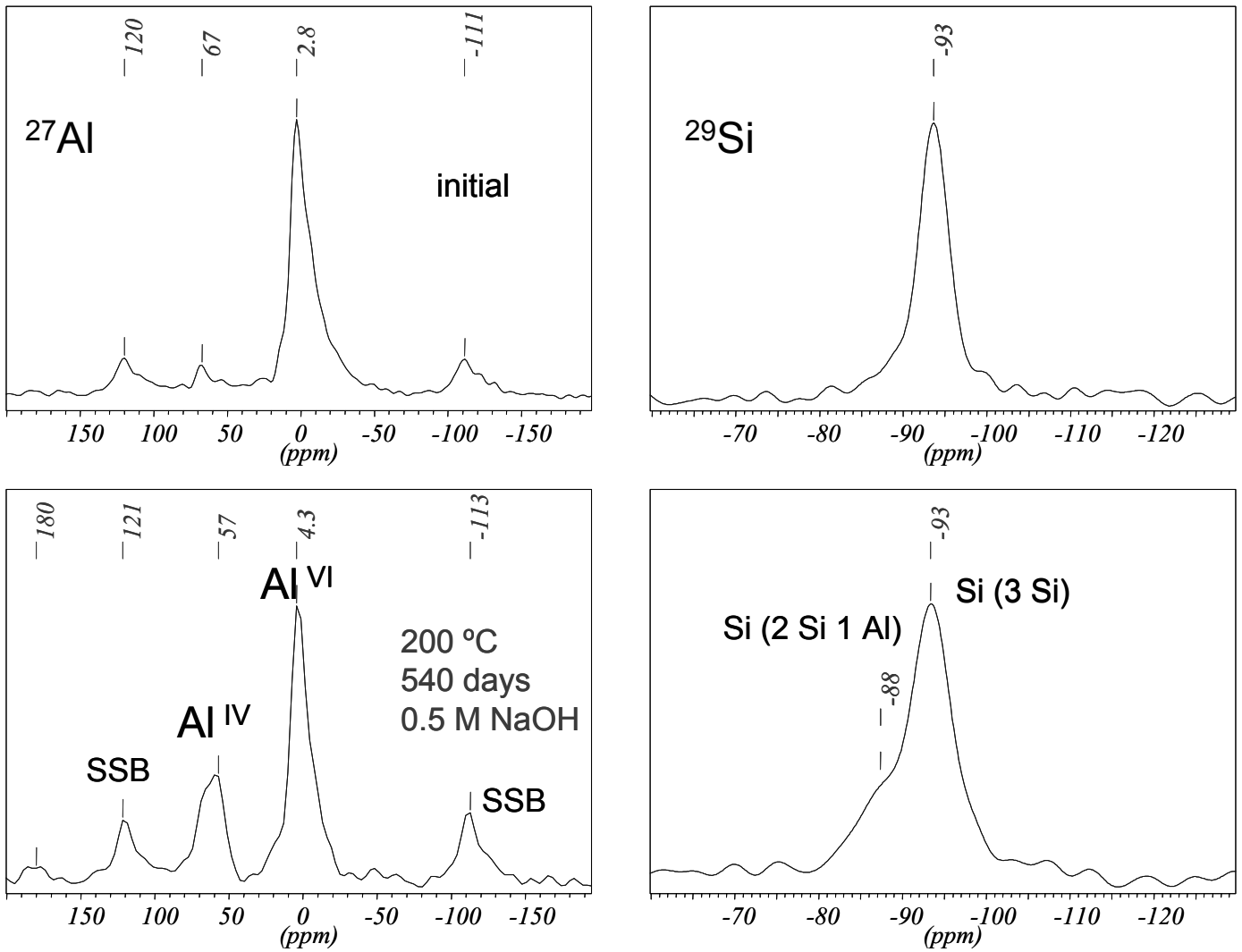
Fig. 10.- $^{29}$Si and $^{27}$Al MAS-NMR spectra of initial and reacted FEBEX bentonite. SSB: Spinning Side Bands.
Fig. 10.- Espectro MAS-NMR de $^{29}$Si y $^{27}$Al de la bentonita FEBEX inicial y después de reaccionar. SSB: Spinning Side Bands.
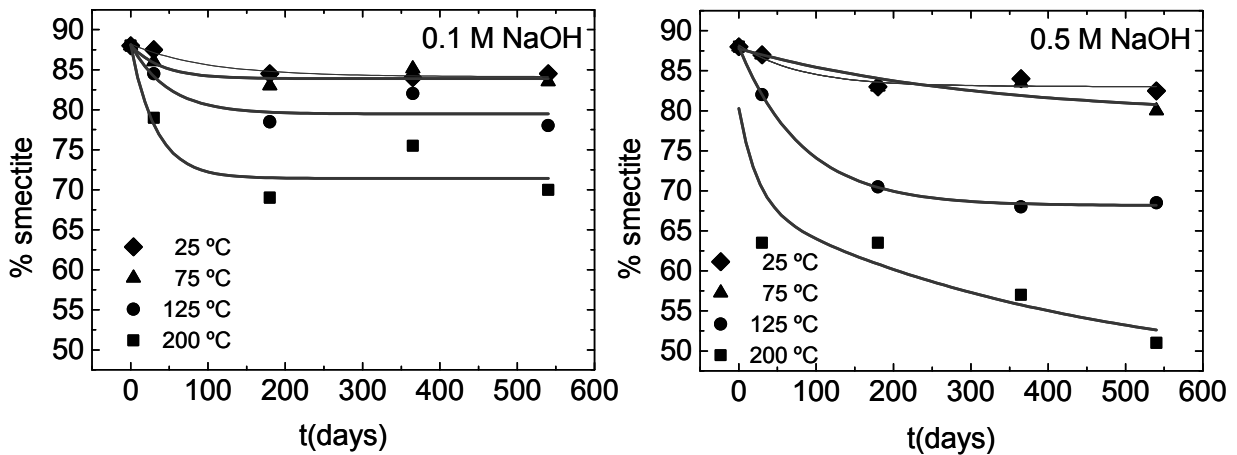


Fig. 11.- Smectite content evolution as a function of time and temperature at 0.1 and 0.5 M NaOH concentrations. Experimental points are fitted to an exponential decay function (y = y0 + A1*exp(-(x-x0)/t)).
Fig. 11.- Evolución del contenido en esmectita en función del tiempo y de la temperatura a concentraciones de NaOH de 0.1 M y 0.5 M. Los puntos experimentales se ajustan a una función exponencial del tipo (y = y0 + A1*exp(-(x-x0)/t)).

| pH | HCO$_3^-$ | SO$_4^{2-}$ | Cl$^-$ | SiO$_2$ (aq) | Na$^+$ | K$^+$ | Mg$^{2+}$ | Ca$^{2+}$ | Total equivalents |
|----|------|------|------|------|------|------|------|------|------|
| 8.1 | 2.27 | 0.18 | 0.39 | 0.84 | 0.52 | 0.03 | 0.33 | 0.92 | 3.024 |

Table 6.- Chemical composition (mmol/l) of the granitic water used in the permeability cell tests.
Tabla 6.- Composición química (mmol/l) del agua granítica usada en los ensayos en celdas de permeabilidad.

| T (ºC) | CEM I-SR | CEM I |
|----|------|------|
| 35 | $0.67 \pm 0.38 \cdot 10^{-11}$ | $1.05 \pm 0.27 \cdot 10^{-11}$ |
| 60 | $1.81 \pm 0.42 \cdot 10^{-11}$ | $1.55 \pm 0.59 \cdot 10^{-11}$ |
| 90 | $4.87 \pm 0.55 \cdot 10^{-11}$ | $1.71 \pm 0.57 \cdot 10^{-11}$ |

Table 7.- Average hydraulic conductivity (m/s) of the cement-bentonite samples as function of the temperature and the cement type.
Tabla 7.- Conductividad hidráulica media (m/s) de las muestras de cemento-bentonita en función de la temperatura y del tipo de cemento.

*Permeability and effluent pH evolution*

The hydraulic conductivity of the cement-bentonite system is obtained by applying Darcy's law to the evolution of the volumetric flow rate observed in the tests. The average results are shown in the Table 7.

The hydraulic conductivity is between $10^{-11}$ and $5 \cdot 10^{-11}$ m/s. These data are similar to the values mentioned in the literature for the compacted bentonite to similar densities and in the same range of temperature (Oscarson *et al.*, 1996; Madsen, 1998; Cho *et al.*, 1999). Therefore, the hydraulic conductivity of the cement-bentonite system is controlled by both materials, taking into account that the hydraulic conductivity for the cement mortar lies within the same order of magnitude

The pH evolution of the effluent during the tests is represented in Figure 13. Although the initial pH of the cement pore-water varied between 13 and 14, during the tests, the pH of the effluents reached a maximum of 11.5, and later was stabilized between 10 and 11. There are not significant variations in the effluent pH as a function of the temperature and the cement type. Moreover, this pH is more consistent with the already mentioned montmorillonite-CSH interaction control than that of the portlandite hydrated cement phase. This is again emphasizing the importance of pH buffering by the bentonite.

*Thickness of alteration in bentonite*

The compacted bentonite (1.5 cm thickness) was sliced in two 0.75 cm sections (interface and bulk sample). The bentonite reached Ca$^{2+}$ saturation at the exchangeable positions (Ca-exch) after six months in the entire 1.5 cm bentonite sample. Furthemore, an excess of Ca-exch (150 – 200 cmol(+)/kg) relative to the known CEC of the ben-

tonite (100 cmol(+)/kg) was systematically observed in the interface sample at 35-60 ºC. This fact, as has been demonstrated later (Sánchez *et. al.*, 2006), indicated the presence of amorphous CSH-gels, that were dissolved in significant amounts during the extraction of exchangeable cations at pH = 8. However, a precise measurement of the thickness affected by this effect could not be determined.

Although zeolites were not found in this compacted bentonite experiments, the incorporation of Mg$^{2+}$ in the smectite observed in the batch experiments, was evident from the structural formula data at 90 ºC. In Table 8, the structural formulae of the smectite at the interface and in the bulk bentonite sections at 90 ºC are shown.

The enrichment in Mg$^{2+}$ at the cement-bentonite interface was measured from the EDX mapping of Mg$^{2+}$ (distribution density) in polished resin-embedded sections of the cement-bentonite samples (Fig. 14). The enriched area was < 0.5 mm in the most altered sample (90 ºC, 12 months).

*2.2.2. Composite mortar/intermediate density compacted bentonite (1.4 g/cm³ dry density)*

In the second approach to reactive transport experiments a column made of 1.4 g/cm³ dry density compacted bentonite was held in contact with an OPC mortar (based on CEM-I). In this case, two alkaline solutions (Ca(OH)$_2$ saturated and NaOH 0.25 M) were injected from the mortar's side at 25, 60 and 120 ºC. Thus, a higher pH regime was imposed at the cement/bentonite interface compared to the first tests. The permeability of the system and the effluent fluid composition were determined periodically, and finally the solid phase was sampled and analyzed after 1 year of treatment.
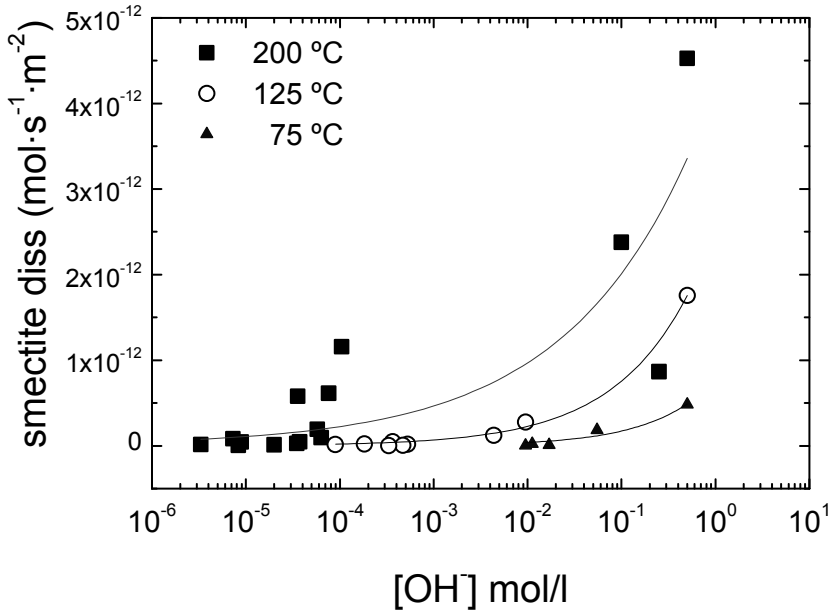
Fig. 12.- $[OH]^{0.5}$ dependent rate laws for the transformation (dissolution) of montmorillonite.

Fig. 12.- Leyes dependientes de la tasa de $[OH]^{0.5}$ para la transformación (disolución) de montmorillonita.

Fig. 13.- pH evolution versus the pore volume $cm^3$ as function of the temperature and cement type in the permeability cell tests.

Fig. 13.- Evolución del pH versus el volumen de poro ($cm^3$) en función de la temperatura y del tipo de cemento en los ensayos en celdas de permeabilidad.
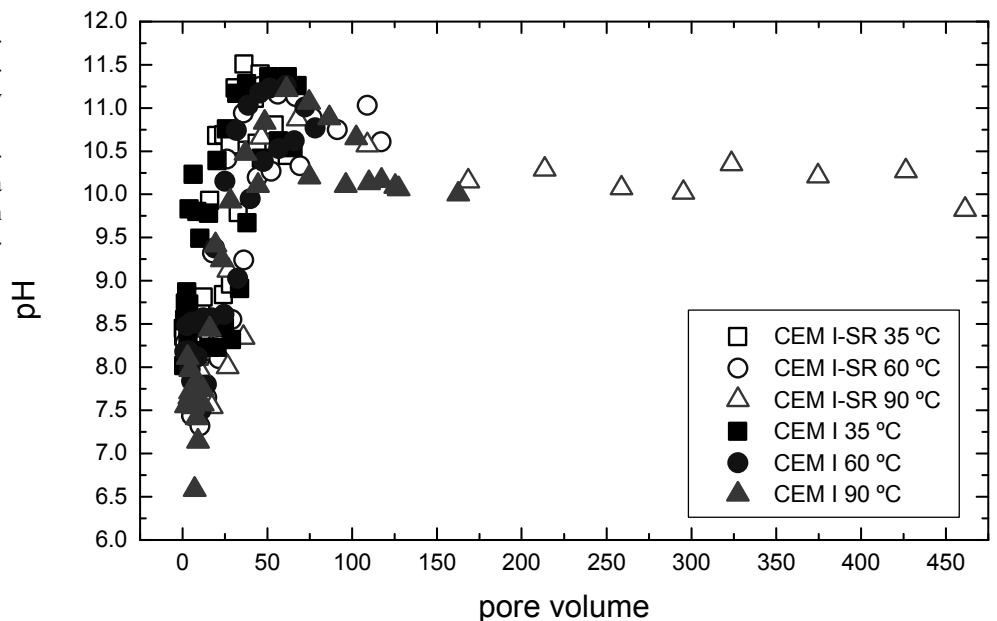


## *Permeability and effluent pH evolution*

The permeability of the cement-bentonite column increased when temperature rose. We observed higher permeability when injecting NaOH solution compared to injecting $Ca(OH)_2$ solution , although values of hydraulic conductivity remained in all cases within the normal values of the 1.4 $g/cm^3$ compacted bentonite of $10^{-13}$ m/s. (Villar and Rivas, 1994) (Table 9). However, at the end of the 120 ºC NaOH experiment (after six months), the hydraulic conductivity rose suddenly to more than twice the value of Table 7. The increase corresponded to a parallel pH increase measured at the effluent port, up to pH 12.3. Table 10 shows a comparison between the chemical parameters measured in the NaOH or $Ca(OH)_2$ experiments at 120 ºC. At lower temperatures, the pH of the effluent in both experiments were always lower than pH = 9. Keeping in mind the previous 1.2 $g/cm^3$ experiments, the lower permeabilities imposed with compaction caused a higher buffering potential due to the longer residence times of interaction of the alkaline fluid with the bentonite clay matrix.

When the experiments were dismantled they were sampled in three slices of 7 mm thickness (the total bentonite thickness was 2.1 cm). In addition to permeability, the pore-size distribution at the mesopore scale was also measured ($N_2$ adsorption-desorption isotherms). Figure 15 shows the pore-size distribution calculated for the slice in contact with the mortar, comparing the two alkaline solutions and the effect of temperature. There was a big devia-

| Cement type | t (months) | section | Tetrahedral sheet | | | Octahedral sheet | | | | | Interlayer | | |
|---|---|---|---|---|---|---|---|---|---|---|---|---|---|
| | | | $Si^{4+}$ | $Al^{3+}$ | charge | $Al^{3+}$ | $Fe^{3+}$ | $Mg^{2+}$ | $Ti^{4+}$ | charge | $Ca^{2+}$ | $K^+$ | charge |
| CEM I-SR | 1 | interface | 7.68 | 0.32 | 0.32 | 2.57 | 0.38 | 1.16 | 0.01 | 0.79 | 0.49 | 0.08 | 1.06 |
| | | bulk | 7.74 | 0.26 | 0.26 | 2.68 | 0.39 | 0.93 | 0.01 | 0.89 | 0.51 | 0.09 | 1.11 |
| | 12 | interface | 7.68 | 0.32 | 0.32 | 2.61 | 0.38 | 1.09 | 0.02 | 0.77 | 0.52 | 0.09 | 1.13 |
| | | bulk | 7.69 | 0.31 | 0.31 | 2.69 | 0.38 | 0.97 | 0.01 | 0.81 | 0.51 | 0.09 | 1.11 |
| CEM I | 1 | interface | 7.72 | 0.28 | 0.28 | 2.67 | 0.40 | 0.98 | 0.01 | 0.79 | 0.48 | 0.09 | 1.05 |
| | | bulk | 7.71 | 0.29 | 0.29 | 2.69 | 0.40 | 0.91 | 0.01 | 0.87 | 0.51 | 0.10 | 1.12 |
| | 12 | interface | 7.67 | 0.33 | 0.33 | 2.59 | 0.37 | 1.13 | 0.01 | 0.82 | 0.52 | 0.09 | 1.13 |
| | | bulk | 7.68 | 0.32 | 0.32 | 2.70 | 0.39 | 0.93 | 0.02 | 0.79 | 0.52 | 0.11 | 1.15 |

Table 8.- Structural formulae of the smectites at 90 ºC as function of the cement type in the permeability cell tests. The structural formulas has been calculated from chemical analysis (FRX) of a < 0.5μm separated clay fraction after homoionization in $Ca^{2+}$.

Tabla 8.- Fórmula estructural de las esmectitas a 90ºC, en función del tipo de cemento, en los ensayos en celdas de permeabilidad. La fórmula estructural se ha calculado a partir del análisis químico (FRX) de una fracción de arcilla <0.5μm separada después de su homoionización en $Ca^{2+}$.

| solution / T(ºC) | 25 | 60 | 120 |
|---|---|---|---|
| NaOH 0.25 M | $(1.59 \pm 4.64) \times 10^{-13}$ | $(4.10 \pm 1.33) \times 10^{-13}$ | $(5.57 \pm 1.53) \times 10^{-13}$ |
| $Ca(OH)_2$ sat. | $(1.52 \pm 6.86) \times 10^{-13}$ | $(2.58 \pm 1.50) \times 10^{-13}$ | $(3.77 \pm 1.72) \times 10^{-13}$ |

Table 9.- Values of hydraulic conductivity, K $(ms^{-1})$.

Tabla 9.- Valores de conductividad hidráulica, K (m/s).

tion of the pore-size profiles and external specific surface measurements associated with the 120 ºC NaOH experiment. The distribution profile shows the clogging of the initial mesoporosity. This process is taking place by the precipitation of secondary minerals (analcime and CSH-gel, to be discussed later). Then, the observed increase of permeability in this test would have to operate by means of the formation of preferential pathways, where the fluid travelled more easily, decreasing in this way the inter-action with the remaining clay buffering phases (the pH was distinctly increased). This may explain the fact that more than 70 % of the initial montmorillonite remained unaltered in this section (Fernández *et al.*, 2006).

*Thickness of alteration in bentonite*

It was possible to measure the spatial extension of mineral reactions in these experiments directly from XRD, SEM-EDX and thin section optical microscopy. In the worst case, and imposing a high pH at the interface, the observed altered rim affecting most of the interface was not thicker than 2 mm. Table 11 summarizes the main

observations related to the more reactive NaOH experiments. Figure 16 shows the SEM aspects of mineral phases listed in Table 11. Figure 17 displays the spatial distribution of the alteration by optical microscopy, and illustrates quite well the measured alteration thickness.

## 3. Contribution to the performance of the FEBEX bentonite barrier at high pH

### 3.1. The particular nature of FEBEX bentonite alkaline reaction products

The experimental alteration of FEBEX bentonite has been studied in batch experiments and column experiments. Batch experiments play a key role in defining which phase can most probably form during the alkaline plume development.

The main phases identified in the alkaline reaction of FEBEX bentonite are phillipsite, Mg-clays, analcime, tobermorite and CSH-gels. It is remarkable that the observed reactions, although initiated at pH 13.5-13.0, con-

| T (ºC) | Pore volume | Time (days) | Na$^+$ | SiO$_2$ | Cl$^-$ | SO$_4^{2-}$ | Alkalinity | pH |
|--------|-------------|-------------|--------|---------|--------|-------------|------------|-----|
| NaOH solution 0.25 M, pH = 13.26 ||||||||||
| 120 | 0.50 | 29 | 43.72 | 0.17 | 21.00 | 13.92 | 1.00 | 7.19 |
| | 1.00 | 51 | 63.56 | 0.42 | 30.24 | 17.48 | 1.08 | 8.00 |
| | 2.00 | 121 | 50.61 | 7.48 | 5.43 | 17.41 | 16.20 | 9.94 |
| | 3.00 | 155 | 69.34 | 18.92 | 2.18 | 4.60 | 64.37 | 11.49 |
| | 4.00 | 189 | 177.35 | 14.80 | 2.18 | 5.90 | 171.89 | 12.32 |
| | 5.00(*) | 212 | 230.78 | 19.17 | 0.92 | 8.81 | 231.60 | 12.44 |
| | 7.00 | 252 | 758.62 | 287.24 | 0.50 | 3.70 | 738.07 | 12.65 |
| | 9.00 | 285 | 373.46 | 94.10 | 0.42 | 1.22 | 388.62 | 12.39 |
| Ca(OH)$_2$ saturated solution, pH = 12.60 ||||||||||
| 120 | 1.00 | 80 | 49.26 | 5.82 | 17.47 | 16.83 | 3.71 | 6.74 |
| | 2.00 | 150 | 31.39 | 0.40 | 4.61 | 14.35 | 2.90 | 8.16 |
| | 3.00 | 203 | 29.62 | 8.59 | 2.05 | 13.84 | 2.02 | 8.62 |
| | 4.00 | 245 | 25.39 | 10.95 | 1.58 | 12.00 | 1.27 | 8.75 |
| | 5.00 | 284 | 21.52 | 4.75 | 1.10 | 7.25 | 3.03 | 9.00 |
| | 6.00 | 317 | 17.03 | 8.60 | 0.74 | 4.70 | 5.22 | 9.46 |
| | 7.00 | 336 | 12.65 | 10.25 | 0.65 | 3.52 | 5.37 | 9.47 |
| FEBEX bentonite ||| 60.69 | 0.17 | 78.13 | 8.96 | 1.29 | 7.34 |

*(\*) The data taken before this pore volume in this experiment did not correspond to the total water amount percolated due to the unexpected increase in permeability that did not allow to measure properly the volume percolated.*

Table 10.- pH and concentration of major aqueous components (mmol/l) at the effluent in the tests carried out at 120ºC. Values are averaged for the same number of bentonite pore volumes.

Tabla 10.- pH y concentración de los componentes acuosos mayores (mmol/l) en el efluente, en los ensayos realizados a 120ºC. Los valores son el promedio para el mismo número de volúmenes de poro de bentonita.
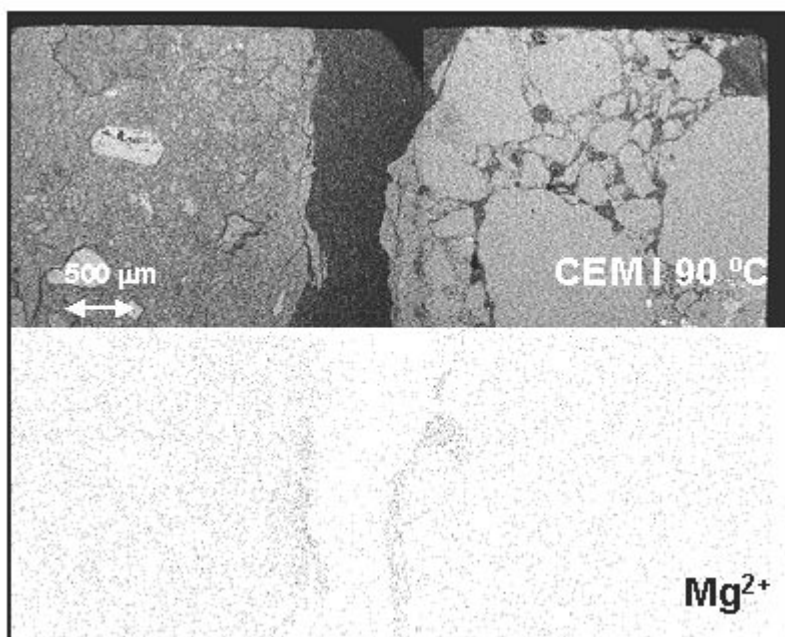


Fig. 14.- SEM image (upper) and EDX mapping (lower) of Mg (point density) in the cement (right)-bentonite (left) interface after a 12 month test at 90 ºC with the cement CEM-I. The black intermediate section is a gap produced during sample preparation.

Fig. 14.- Imagen de microscopio electrónico de barrido (superior) y mapa de difracción de rayos X (inferior) de Mg (densidad de puntos) en la interfase cemento (derecha) - bentonita (izquierda) después de un ensayo de 12 meses a 90ºC con el cemento CEM-I. La sección intermedia negra es un hueco formado durante la preparación de la muestra.
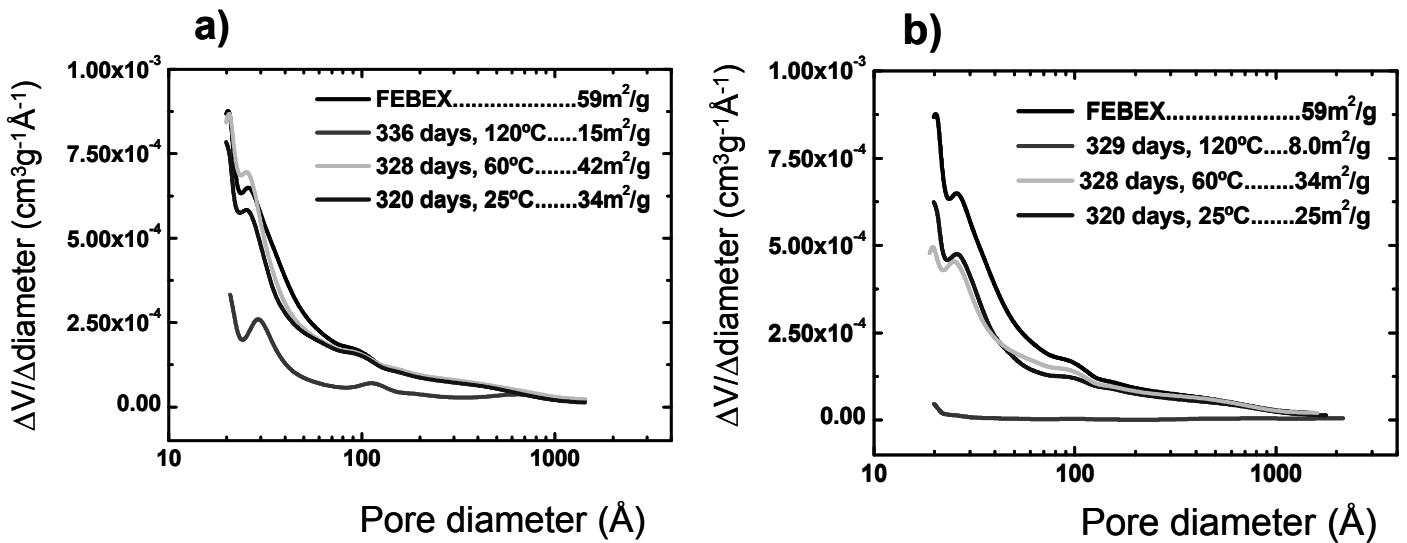
**a)**



**b)**



Fig. 15.- Pore size distribution and BET surface in initial FEBEX bentonite and section 1 (interface) of alterated bentonite. a) Ca(OH)$_2$ saturated solution; b) NaOH 0.25 M solution. Pores size distribution has been determined by N$_2$ adsorption (> 50 data points), using the BJH equation. DV/DF: increment of volume (N$_2$ at standard pressure) to diameter increment ratio.

Fig. 15.- Distribución de tamaño de poro y superficie BET en la bentonita FEBEX inicial y en la sección 1 (interfase) de la bentonita alterada. a) Solución saturada en Ca(OH)$_2$; b) Solución 0.25 M de NaOH. La distribución de tamaño de poro se ha determinado por adsorción de N$_2$ (>50 puntos), usando la ecuación BJH. DV/DF: relación entre el incremento de volumen (N$_2$ a presión estándar) y el aumento de diámetro.

tinued to operate at lower pH, as far as the precipitation of the newly-formed phases is concerned.

At temperatures between 25 - 90 ºC, relevant for the performance assessment (PA) of DGR-HLRW, the reaction pH stayed in the range of 12.5 to 10.5 as a function of decreasing initial pH or rising of temperature. Zeolites are produced at pH higher than 12.0 in this range, but magnesium smectite can be produced at lower pH values. It is interesting to note that in batch experiments, when portlandite is introduced in the system, the characteristic reactive process of zeolite and Mg-clay formation is shifted to higher temperatures.

Phillipsite precipitates rather than analcime when sodium activities decrease. In any case, these zeolites are the only phases experimentally observed. It is worth to note that the chemical composition of these zeolites is very similar to that found by Chipera and Bish (1997). We recommend the use of their thermodynamic data for these phases, which is supported by our findings that using these data the zeolites are becoming more supersaturated in the reaction solutions (Cuevas, 2005).

| Mineral phase | T (ºC) /pH at 2.1 cm from the interface | altered bentonite thickness (mm) |
|---|---|---|
| Zeolites (analcime) | 25 - 60ºC,  pH = 8 - 9<br>120ºC,      pH = 12 | < 0.1<br>1.5 – 20 (*) |
| Mg-smectite | 25 - 60 ºC,  pH = 8 - 9<br>120ºC      pH =  12 | < 0.1<br>0.0 – 10 |
| Brucite | 25 - 60ºC,  pH = 8 - 9 | < 0.1 |
| CSH Ca/Si (1.0 – 0.6) | 25 - 60ºC,  pH = 8 - 9<br>120ºC      pH = 12 | < 0.1<br>< 1.5 |

(*) the weight percent of analcime reached at maximum 16 % in the interface zone, although at 2.1 cm from the interface, proportions up to 5 % were measured.
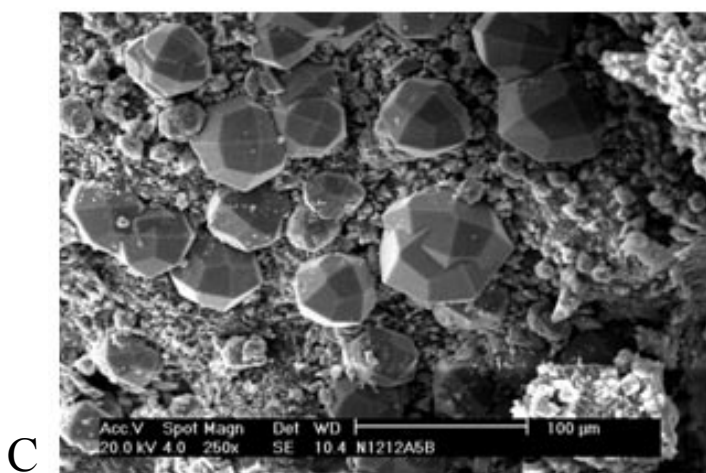
Table 11.- Spatial distribution of alteration in the bentonite column after 300 days in the NaOH percolating experiment.

Tabla 11.- Distribución espacial de la alteración en la columna de bentonita después de 300 días, en el experimento de percolación de NaOH.
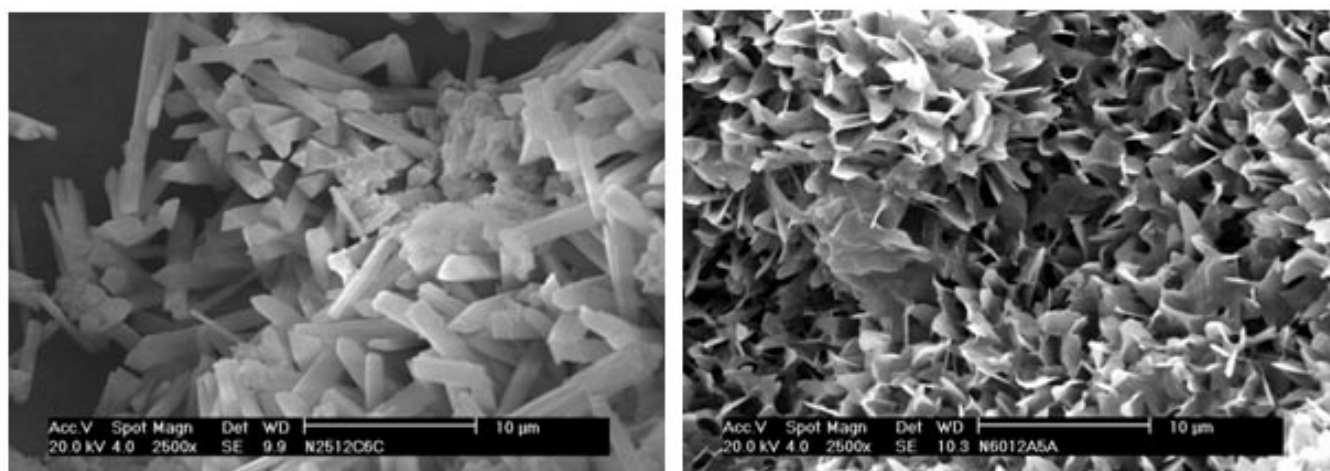
Fig. 16.- SEM Photographs. A:. Triangular prisms of brucite, NaOH 0.25 M, 25 ºC; B: Laminar CSH-gel of tobermorite type (Ca/Si = 0.8), NaOH 0.25 M, 60 ºC; C: Isometric analcime on clay surface, NaOH 0.25 M, 120 ºC.

Fig. 16.- Fotografías de microscopio electrónico de barrido. A: Prismas triangulares de brucita, NaOH 0.25 M, 25 ºC; B: Gel CSH laminar de tipo tobermorita (Ca/Si = 0.8), NaOH 0.25 M, 60 ºC; C: Analcima isométrica sobre superficie de arcilla, NaOH 0.25 M, 120 ºC.

The formation of a smectitic trioctahedral phase has been confirmed, so that the use of saponite-stevensite phases is justified in the modeling exercises. However, some uncertainty remained about the nature of CSH phases formed at low temperature. They are amorphous and it is not possible to distinguish separately calcium silicates and clay materials. We have presumed they should be similar in composition to the fibrous or small crystalline calcium-silicate aggregates formed at 125 ºC. The more frequent Ca/Si ratios were 0.6 -1.0, close to tobermorite-like phases. Some aluminum is present in these phases, and therefore the existence of CA(aluminate)SH phases may have to be taken into account in future modeling work.

## 3.2. The reaction rate of FEBEX montmorillonite at high pH: a quantitative mineralogical approach.

The kinetics of mineral formation (zeolites and Mg-clays) and smectite transformation have been evaluated. The reaction rate for analcime formation has the form $R(mol \cdot s^{-1}) = A \ (m^2) \cdot k \ [OH^-]^{0.3}$ at 200-125 ºC. The apparent activation energy has been calculated also: $\ln k = (-12.23) - (5176) * (1/T)$; $E_a = 43$ kJ/mol. (Sánchez *et al.*, 2006). These data are consistent with a dissolution-precipitation process in tectosilicates, but it is very similar to that of the montmorillonite transformation. This similarity is interpreted as the confirmation of a common limiting process prevailing in both reactions: the montmorillonite dissolution.
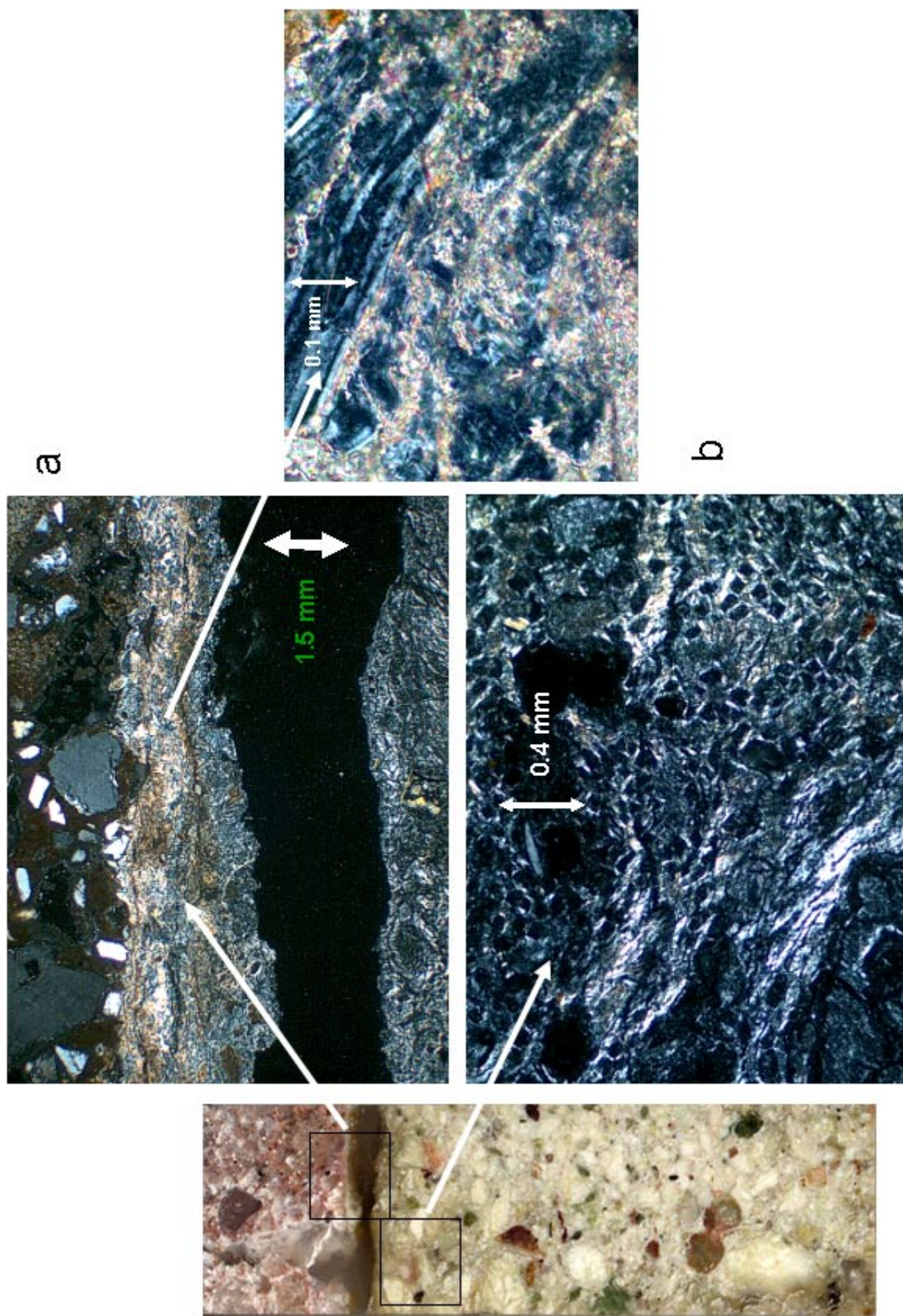
Fig. 17.- a: Bright layer (calcium phases) at the interface mortar-bentonite. The horizontal black gap is due to a preparation artefact. b: isotropic cubic shapes (analcime) surrounded by thin films of oriented clays as seen by optical microscopy in thin section. NaOH 0.25 M, 120 °C.

Fig. 17.- a: Capa brillante (fases de calcio) en la interfase mortero-bentonita. El hueco negro horizontal es debido a un artefacto en la preparación de la muestra. b: Formas cúbicas isotrópicas (analcima) rodeadas por finas películas de arcillas orientadas, bajo el microscopio óptico en lámina delgada. NaOH 0.25 M, 120 °C.
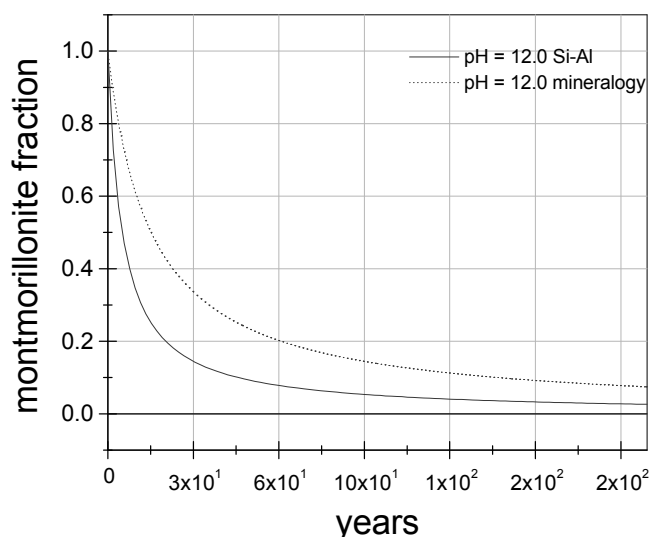
Fig. 18.- Conversion time for 100 g of bentonite (dissolution of montmorillonite).

Fig. 18.- Tiempo de transformación de 100 g de bentonita (disolución de montmorillonita).

| | Rate (mol m$^{-2}$s$^{-1}$) |
|---|---|
| Mineralogical data | $4.02 \cdot 10^{-14}$ |
| Si-Al dissolution data | $1.18 \cdot 10^{-13}$ |

Table 12.- Reaction rate for FEBEX montmorillonite dissolution at 50 ºC and pH = 12.5.

Tabla 12.- Tasa de reacción para la disolución de la montmorillonita FEBEX a 50ºC y pH = 12.5.

The rate of dissolution of montmorillonite has been calculated from the mineralogical quantification of smectite in the 75 – 200 ºC tests. The overall kinetics for the conversion of montmorillonite is in very close agreement with the rate of dissolution of montmorillonite at pH = 9 obtained by Cama *et al*. (2000) using FEBEX smectite at 80 ºC. Moreover, the order of reaction is in agreement with the values obtained by Huertas *et al*. (2004) at 25 - 50 ºC, pH > 11, reported in the Ecoclay-II final scientific report. These studies used the analysis of silica or alumina in solution in order to evaluate the rate of the dissolution of montmorillonite. The consistency found between this data and the data obtained form mineralogical quantification can be considered as a validation criteria for the kinetic rate law, although some discrepancy is found in the values of the rate constants. Anyway, this issue can be tested in reaction and transport predictive models.

Table 12 compares kinetic results obtained by means of a mineralogical transformation rate (Sánchez *et al*., 2006) and by a Si-Al dissolution rate (Huertas *et al*.,2004). The calculation has been performed at 50 ºC, which will be the average temperature in the system during several hundred years. A constant pH of 12.0 has been also considered as this is the stationary pH when a pH 13.5 alkaline solution is held in contact with FEBEX bentonite. The reaction rate calculated by Si-Al dissolution is one order of magnitude higher, a fact that can be explained by the differences in solid to solution ratios that are 100 times higher in the batch experiments (1/3) compared to the flow-through experiments (1/110). The most readily accessible area will produce higher rates, and even lower reaction rates can be envisaged in the alteration of compacted bentonites. Figure 18 takes into account both approaches for the dissolution of 100 g of bentonite. It must be mentioned that another factor to reduce the reaction rate is the proximity to equilibrium conditions, favoured at higher solid to solution ratios.

An important consequence for the PA issues is that when scaling our batch experiments, the volume of solution is the pore-volume of a square column (30 cm height) of a typical OPC concrete acting on 100 g of bentonite forming a 0.6 cm thick layer of compacted bentonite (1.65 g/cm$^3$ of dry density). In addition, a 0.5 M alkali solution comprises to the total potential alkalis (K,Na-OH) present in the concrete. This means that a thin layer of bentonite is able to buffer considerably the initial hyper-alkaline plume: i.e form pH 13.5 to pH: 12 at 75 ºC. The conversion time estimation (80 % of 100 g transformation takes 20 years (Si-Al model) to 60 (mineralogy model) years) seems to be very short. One must take into account that the reaction rate will diminish as the progress of the reaction is approached towards equilibrium, and this is more easily achieved when the solid to solution ratios are large, as is the case for compacted bentonite. Again, transport and reaction models can serve to account for these effects.

### 3.3. The experimental validation of FEBEX bentonite reactivity in column experiments.

Column experiments are necessary for model validation to obtain data that are directly applicable to reactive transport models. The formation of CSH-gel has been validated at the cement-bentonite interface in the column experiments including OPC cement mortar and compacted bentonite at 25-120 ºC with either granitic, Ca(OH)$_2$ (saturated) or NaOH 0.25 M as percolating fluids. The NaOH experiments were more demonstrative, and the alteration of the bentonite sample was insignificant with a Ca(OH)$_2$ solution.

The location of CSH is very restricted to a film (< 0.1 mm) at the mortar-bentonite interface at 25–60 ºC, where tobermorite-like gels, Mg-Clays and brucite were observed. On the other hand, at 120 ºC a thicker film of CSH-gel (1-1.5 mm) was developed. Analcime was observed locally at the interface at 25-60 ºC, but it is massively produced at 120 ºC, always beyond the CSH-layer. The CSH-gel layer is more or less continuous, but the analcime microcrystals are present in discrete areas with a heterogeneous distribution. In conclusion, the alteration front is not homogeneous. The surface area of the bentonite after this alteration decreased below 2000 $m^2$/kg indicating that some clay aggregates have been cemented. This means that the smectite effective surface area for dissolution has to be corrected at least by a factor of 10, or instead, some stagnant zones can be created in the reaction and transport models.

Another consequence for the opening of preferential fluid path ways and of the reduction of reactive surfaces is that a hyper-alkaline front will extend deeper into the bentonite by a factor of 10 and will affect several cm (5-10 cm) instead the 0.5 cm as argued using the results from the batch experiments. However, this observation is based on observations at high temperatures.

These results are very valuable as some models developed on reactive transport by alkaline fluids in bentonite or argillites predict the formation of a tobermorite layer which induces a porosity closure immediately after the cement interface, where magnesium phases are also formed: celadonite and brucite. Some models propose a silica dissolution front and the formation of analcime after the CSH zone and the formation of a Ca-Zeolite after the CSH-zone. The porosity closure predicted in these models is in agreement with the severe reduction in permeability in the 25 ºC higher density column tests. However, despite of the CSH layer produced in the 120 °C NaOH column, permeability did rise. The reason is that preferential pathways of alteration are opened at high temperature due to a significant degree of montmorillonite dissolution (Fernández *et al*., 2006).

## Acknowledgements

## References

Adler, M. (2001): *Interaction of Claystone and Hyperalkaline Solutions at 30 ºC: A combined Experimental and Modeling Study*. Ph D. Thesis. University of Berne.

Andersson, K, Allard, B., Bengtsson, M., Magnusson, B. (1989): Chemical composition of cement pore solutions. *Cement and Concrete Research*, 19: 327-332.

ANDRA (2005): Ecoclay II : Effects of Cement on Clay Barrier Performance - Phase II. Final Report. EC project n°FIKW-CT-2000-00028; Andra report.n°CRPASCM04-0009, 381 p.

Bauer, A., Berger, G. (1998): Kaolinite and smectite dissolution rate in high molar KOH solutions at 35 ºC and 80 ºC. *Applied Geochemistry*, 33: 905-916.

Bauer, A., Velde, B. (1999). Smectite transformation in high molar KOH solutions. *Clay Minerals*, 34: 259-273.

Berner, U.R. (1992): Evolution of pore water chemistry during the degradation of cement in a radioactive waste repository environment. *Waste Management*, 12: 201-219.

Bradbury, M.H., Baeyens, B. (2003): Porewater chemistry in compacted re-saturated MX-80 bentonite. *Journal of Contaminant Hydrology,* 61: 329–338.

Caballero, E., Fernandez-Pôrto, M.J., Linares, J., Reyes, E. (1983): Las bentonitas de La Serrata de Níjar (Almería). Mineralogía, geoquímica y mineralogénesis. *Estudios Geológicos*, 39: 121-140.

Caballero, E., Jiménez de Cisneros, C., Huertas, F.J., Huertas, F., Pozzuoli, A., Linares, J. (2005): Bentonites from Cabo de Gata, Almería, Spain: a mineralogical and geochemical review. *Clay Minerals*, 40: 463-480.

Cama, J., Ganor, J., Ayora, C., Lasaga, A. (2000): Smectite disssolution kinetics at 80ºC and pH 8.8. *Geochimica et Cosmochimica Acta*, 64: 2701-2717.

Chipera, S.J., Bish, D.L. (1997): Equilibrium modeling of clinoptilolite–analcime equilibria at Yucca Mountain Nevada USA. *Clays and Clay Minerals*, 45: 226-239

Chermak, J.A. (1992): Low experimental temperature investigation of the effect of high pH NaOH solutions on the Opalinus Shale, Switzerland. *Clays and Clay Minerals*, 40: 650-658

Cho, W.J., Lee, J.O., Chun, K.S. (1999): The temperature effects on hydraulic conductivity of compacted bentonite. *Applied Clay Science*, 14: 47-58.

Cobeña, J.C., Martín, M., Ramírez, S., Vigil de la Villa, R., Cuevas, J., Leguey, S. (1998): Estudio detallado de la mineralogía y microestructura de una bentonita compactada sometida a procesos de calentamiento e hidratación. *Boletín de la Sociedad Española de Mineralogía*, 21-A: 66-67.

Cuadros, J., Linares, J. (1995): Some evidence supporting the existence of polar layers in mixed-layer illite/smectite. *Clays and Clay Minerals*, 43: 467-473.

Cuevas, J., Sánchez, L., Fernández, R., Vigil de la Villa, R., Ruiz de León, D., Ramírez, S., Leguey, S. (2004): Transformación de montmorillonita a saponita en condiciones alcalinas a 75-200 ºC. *Macla*, 2: 105-106.

Cuevas, J. (2005): Geochemical reactions in FEBEX bentonite. In: ANDRA (ed.): *Ecoclay II: Effects of Cement on Clay Barrier Performance - Phase II*. Final Report. EC project n°FIKW-CT-2000-00028; Andra report. n° CRPASCM04-0009, 381 p.

Cuevas, J., Fernández, R., Sánchez, L., Ruiz de León, D., Vigil de la Villa, R., Leguey, S. (2006): Interacciones a corto y largo plazo en una barrera mineral compuesta por hormigón y bentonita. In: M. Suárez, M.A. Vicente, V. Rives, M.J. Sánchez (eds.) : *Materiales Arcillosos: de la Geología a las Nuevas Aplicaciones*". Sociedad Española de Arcillas. Salamanca: 197-207.

De Windt, L., Pellegrini, D., van der Lee, J. (2004): Coupled modelling of cement/claystone interactions and radionuclide migration. *Journal of Contaminant Hydrology,* 68: 165-182.

Dove P.M. (1995): Kinetic and thermodynamic controls on silica reactivity in weathering environments. In: A.F. White, S.L. Brandtley (eds.): *Chemical weathering rates of silicates minerals*. Mineralogical Society of America. *Reviews in Mineralogy*, 31: 235-290.

Eberl, D.D., Velde, B., McCormick, T. (1993): Synthesis of illite-smectite from smectite at earth surface temperatures and high pH. *Clay Minerals*, 28: 49-60.

Eijk, v R.J., Brouwers, H.J.H. (2000): Prediction of hydroxil concentrations in cement pore water using a numerical cement hydration model. *Cement and Concrete Research*, 30: 1801-1806.

Faucon, P., Adenot, F., Jacquinot, J.F., Petit, J.C., Cabrillac, R., Jorda, M. (1998): Long-term behavior of cement pastes used for nuclear waste disposal: review of physico-chemical mechanisms of water degradation. *Cement and Concrete Research*, 28: 847-857.

Fernández, R., Cuevas, J., Sánchez, L., Vigil de la Villa, R., Leguey, S. (2006): Reactivity of the cement–bentonite interface with alkaline solutions using transport cells. *Applied Geochemistry*, 21: 977-992.

Fernández, A.M, Baeyens, B., Bradbury, M, Rivas, P. (2004): Analysis of the pore-water chemical composition of a Spanish bentonite used in an engineered barrier. *Physics and Chemistry of the Earth*, 29: 105-118.

Hidalgo, A., Alonso, C., Andrade. C., Fernández, L. (2003): *ECOCLAY II. Review of concrete formulations actually defined for radioactive repositories waste*. WP2. IETCC (CSIC). Madrid. Spain. Interim report.

Hidalgo, A., Castellote, M., Alonso, M.C., Llorente, I., Andrade, C. (2004): Interacción cemento-bentonita en repositorios de alta actividad (proyecto ECOCLAY-II). Tarragona. *V^{as} jornadas de Investigación, Desarrollo tecnológico y Demostración para la Gestión de Residuos Radiactivos*. ENRESA. Publicación técnica 05/2004.

Huertas, F.J., Rozalén, M., García, S., Iriarte, I., Linares, J. (2004): Interacción cemento-bentonita en repositorios de alta actividad (proyecto ECOCLAY-II). Tarragona. *V^{as} jornadas de Investigación, Desarrollo tecnológico y Demostración para la Gestión de Residuos Radiactivos*. ENRESA. Publicación técnica 05/2004.

Huertas, F., Griffault, L., Leguey, S., Cuevas, J., Ramírez, S., Vigil de la Villa, R., Cobeña, J., Andrade, C., Alonso, M.C., Hidalgo, A., Parneix, J.C., Rassineux, F., Bouchet, A., Meunier, A., Decarreau, A., Petit, S., Vieillard, P. (2000): *Effects of cement on clay barrier performance*. Final Report. Ecoclay project. Nuclear Science and Technology. European Commission. EUR 19609. 140p.

Glasser, F.P. (2001): Mineralogical aspects of cement in radioactive waste disposal. *Mineralogical Magazine*, 65: 621-633.

Glasser, F.P., Atkins, M. (1994): Cements in radioactive waste disposal. *Materials Research Society Bulletin*, 12: 33-39.

Linares, J. (1987): Chemical evolutions related to the genesis of hydrothermal smectites (Almería, SE SPAIN). In: R. Rodríguez-Clemente, Y. Tardy (eds.): *Geochemistry and mineral formation in the earth surface*. CSIC-CNRS. Madrid. 567-584.

Linares, J., Huertas, J. Reyes, E., Caballero, E., Barahona, E., Guardiola, J.L., Yáñez, J., Romero, E., Delgado, A., Rodríguez, J., Martín-Vivaldi, M.T. (1993): *Investigación de bentonitas como materiales de sellado para almacenamiento de residuos radiactivos de alta actividad*. ENRESA. Publicación técnica 01/93.

Madsen, F.T. (1998): Clay mineralogical investigations related to nuclear waste disposal. *Clay Minerals*, 33: 109-129.

Nakayama, S., Sakamoto, Y., Yamaguchi, T., Akai, M., Tanaka, T., Sato, T., Iida, Y. (2004): Dissolution of montmorillonite in compacted bentonite by highly alkaline aqueous solutions and diffusivity of hydroxide ions. *Applied Clay Science*, 27: 53-65.

Oscarson, D.W., Dixon, D.A., Hume, H.B. (1996): Mass transport through defected bentonite plugs. *Applied Clay Science*, 11: 127-142.

Ramírez, S., Cuevas, J., Vigil, R., Leguey, S. (2002): Hydrothermal alteration of «La Serrata » bentonite (Almería, Spain) by alkaline solutions. *Applied Clay Science*, 21: 257-269.

Ramírez, S., Vieillard, P., Bouchet, A., Cassagnabère, A., Meunier, A., Jacquot, E. (2005): Alteration of the Callovo–Oxfordian clay from Meuse-Haute Marne underground laboratory (France) by alkaline solution. I. A XRD and CEC study. *Applied Geochemistry*, 20: 89-99.

Read, D., Glasser, F.P., Ayora, C., Guardiola, M., Sneyers, A. (2001): Mineralogical and microstructural changes accompanying the interaction of Boom Clay with ordinary Portland cement. *Advances in Cement Research*, 13: 175-183.

Sánchez, L., Cuevas, J., Ramírez, S., Ruiz de León, D., Fernández, R., Vigil de la Villa, R., Leguey, S. (2006): Reaction kinetics of FEBEX bentonite in hyperalkaline conditions resembling the cement–bentonite interface. *Applied Clay Science*, 33: 125-141.

Savage, D., Noy, D., Mihara, M. (2002): Modelling the interaction of bentonite with hyperalkaline fluids. *Applied Geochemistry*, 17: 207-223.

Savage, D. (1997): *Review of the potential effects of alkaline plume migration from a cementitious repository for radioactive waste. Implications for performance assesment*. UK Environmental Agency. Technical Report. 60p.

Steefel, C.I., Lichtner, P.C. (1994): Diffusion and reaction in rock matrix bordering a hyperalkaline fluid-filled fracture. *Geochimica Cosmochimica Acta*, 58: 3595-3612.

Stumm, W. (1992): *Solid-water interface. Processes at the mineral-water and particle-water interface in natural systems*. John Willey. New York: 428p.

Taylor, H.F.W. (1987): A method for predicting alkali ion concentrations in cement pore solutions. *Advances in Cement Research*, 1: 5-16.

Thomas, W.G. (1982): Exchangeable cations. In A. L. Page, R. H. Miller, D. R. Keeney (Eds). *Methods of Soil Analysis, Part 2*. Chemical and Microbiological Properties (2nd Edition). *Soil Science Society of America*: 159-165.

Vigil, R., Cuevas, J., Ramírez S., Leguey S. (2001): Zeolite formation during the alkaline reaction of bentonite. *European Journal of Mineralogy*, 13: 635–644.

Villar, M.V., Rivas, P. (1994): Hydraulic properties of montmorillonite-quartz and saponite-quartz mixtures. *Applied Clay Science*, 9: 1-9.

Wolery, T.J. (1998). *EQ3/6 Version 7.2c. Software for geochemical modelling*. Lawrence Livermore National Laboratory.